DEFENSIO PER SCIENTIAM

Arctic Ambient Noise

Beamforming and Modelling

Michael Greening

JASCO Research Ltd.

Sidney, B.C.

for

Canada

ARCTIC AMBIENT NOISE
BEAMFORMING AND MODELLING

By

Michael Greening

JASCO Research Ltd.,
Sidney, B.C.

March 1989

ABSTRACT

The following report details the work completed to date in characterizing the transients contained in the acoustic noise produced from Arctic pack ice. A simple source detection system capable of finding transients with a high signal to noise ratio was used and an average and median number of transients of 4 and 2 respectively were found per 2-minute sample of data. These transients were shown to be vertically directional with a loss at 50-100Hz of approximately 15dB from 5 to 15 degrees from horizontal and a further loss of 10dB from 15 to 90 degrees. This vertical directivity was also shown to increase slightly with frequency. In examining bottom characteristics to aid in modelling the source propagation, sub-bottom layers at 3m and 15 m deep were found. Although exact measurements of bottom roughness were not obtained, it was observed to be acoustically flat for frequencies of up to 2000Hz.

DATA COLLECTION.

A set of approximately 100 two-minute samples of Arctic background noise has been extracted from data collected by Defence Research Establishment Pacific and is examined in this report. The data was collected on the pack ice off the continental shelf of the northern coast of Ellesmere Island from April 9, 1988 to April 22, 1988. A vertical array of 24 hydrophones along with a 7 hydrophone horizontal array was deployed in water of 420m depth. The vertical array was linear equispaced with a hydrophone separation of 12m while the horizontal array was a nonequispaced L shape of two different configurations as shown in figure 1. A sampling rate of 516Hz was used and the data was low pass filtered at just below the Nyquist frequency.

SOURCE DETECTION AND DESCRIPTION

Detection of a transient source in a noisy background is a complex and common problem in most fields of acoustics and many techniques are available depending on the source and background characteristics. However, due to the high signal to noise ratio desired for further processing suchh as determining source directivity, a simple and fast detection technique could be used. The technique used was to scan the entire length (generally 2 minutes) of a single channel of a data file to determine the average voltage peak height, and then rescan the channel recording the position of all peaks greater than some user supplied multiple of the average peak height. The mean and median number of sources found with a peak height of greater than 5 times the average was approximately 4 and 2 respectively per 2-minute sample of data.

Figures 2 - 7 show the output of the vertical array for three close range (500m or less) and three far range (3000m to 4000m) transients with peak heights from approximately 7 to 40 times the average peak height. (The ranges for these sources were determined using a ray tracing technique as described later.) All these figures clearly show multipath arrivals corresponding to a direct path, bottom reflection, bottom and surface reflection and multiple reflections from the bottom and surface. Both the low energy transients from close or far range are still easily distinguished when seen on multiple channels. However, a few false alarms (peaks for which no structure was evident across the array) were also detected and the number of false alarms increased rapidly as the ratio of transient peak height to average peak height decreased. Thus, the above values for mean and median number of transients per time do not include the very weak sources and a better technique which has a low rate of false alarm is required. This is being examined in another project (Zakarauskas and Parfitt).

In figures 3 and 4, the energy in the bottom and bottom-surface reflections is comparable with that of the direct arrival, while for figure 2, the energy of the direct arrival is much larger than the bottom or bottom-surface reflections. This is because the transient in figure 2 is close enough that the grazing angle for the bottom reflection is larger than the critical angle.

In figure 3 the energy of the direct arrival obviously increases for the deeper hydrophones. However, the propagation loss for the deeper hydrophones is larger due to increased spreading loss (absorption is negligible at these frequencies and distances), and thus the source must be directional (not a monopole) with more energy transmitted vertically than horizontally into the water column. This is observed for all of the distant transients for which the bottom or multiple arrivals contain more energy than the direct arrival.

From the close range transients, it is seen that the energy in a given arrival (i.e. direct, bottom or bottom-surface reflections) decays to the background level in 0.1 to 0.4 seconds depending on the ratio of peak height to background level. This is in contrast with the distant sources for which the energy of a given arrival does not decay to the background level before the appearance of the next arrival. Also, from the transients shown, it is seen that the energy of a given transient (including all multiple reflections) decays to the background level in approximately 0.5 to 1.0 seconds.

Some of the close range transients exhibited a "precursor" which appeared before the direct arrival as shown in figure 8. The true acoustic wave direct arrival was identified by matching its time delays with the bottom and surface reflections. This precursor occurred in all the high power close range transients except for those closer than about 60m range and was visible in one transient of over 1200m range. Analysis with the horizontal array showed that the precursor always came from the same azimuth as the transient it pre-arrived. At first, it was assumed that these arrivals corresponded to the scattering of ice-trapped energy into the water column by discontinuities in the ice. Under this assumption, the velocity of propagation in the ice was calculated as 3200 +/- 150 m/sec which corresponds with the symmetric plate wave with a measured speed of 3170 m/sec. However, later analysis showed that these precursors all appeared to arrive from the same range regardless of azimuth direction. It was also shown that the calculated time delays for hydrophones at the very top and bottom of the vertical array did not fit the observed delays as accurately as when calculated for the true direct or reflected paths. Because of the apparent equal range and the small error in fit for the time delays when a point source is assumed, it is now believed that these precursors correspond to energy which is leaked from the symmetric plate wave at a constant angle. The exact arrival times and plate wave speed for this situation has not been calculated yet

and should be performed in future work; however, they should not differ much from the values calculated under the first hypothesis.

SOURCE LOCALIZATION

A method of localizing the source (finding the range and bearing) was developed to determine if the sources are randomly distributed or are concentrated in specific areas.

The range of a source was determined using the ray tracing model, SONAR, supplied by Ocean Acoustics. This ray model calculates the eigenrays (the acoustic rays joining a source to a target) for a range independent, vertically stratified fluid with a flat bottom and surface. The measured sound speed profile along with the approximate profile used for the ray model are shown in figure 9 while figure 10 shows the eigenrays joining a surface source at a range of 5000m to the 294m deep hydrophone. The eigenrays for all hydrophones in the vertical array and for ranges 10m to 500m in 10m steps, 520m to 1000m in 20m steps and 1050m to 5000m in 50m steps were computed and the arrival times stored in a file. These arrival times are then matched to the array output to determine the source range. Although some sources were detected at ranges beyond 5000m, these were weak and few in number and are also difficult to localize because of the large overlap of the various paths. Figures 11 and 12 show the array response for a close and distant source respectively along with the calculated arrival times for the various paths (vertical bars). The vertically aligned arrival times for the distant source (at 0.5 sec) correspond to imaginary eigenrays which model energy scattered into shadow zones. At present, determining the source range still requires user intervention to visually match the SONAR calculated arrival times with the array output

and is thus a very slow process. Only about 20 sources have been examined to date. If a transient detector capable of finding the starting point of individual arrivals in a transient source is produced (Zakarauskas and Parfitt), then source range determination can be automated and the range of all transients in all the data files can be determined.

The bearing of a source was determined by matching the arrival times for only the direct arrival on the horizontal array with times calculated using straight ray theory. The ray tracing model was not used to determine bearing because the arrival times on the horizontal array are a function of both bearing and range. Thus, either a very large file containing the arrival times for all bearings and all ranges would be required or the arrival times would have to be calculated interactively to match with the array output. Due to the difficulty in interfacing the ray model with the array output, it was decided to calculate the arrival times interactively using straight ray theory instead. Tests at several angles for both close and far range showed a maximum difference of ten data points between the straight ray and vertically stratified models across the entire array for a source at 100m range. This was reduced to within one data point for a source at 500m range. Thus, except for the very close sources (up to 100m or 200m range), the straight ray theory should provide a very accurate fit to the array response of a transient. For the close sources, the bearing can still be determined by using the end of the array where the hydrophones are more closely spaced. Figures 13 and 14 show the horizontal array output and the calculated arrival times for the same transients shown in figures 11 and 12. Again, determining the source bearing requires user intervention and a proper transient detector (as mentioned above) would be a useful aid.

To date not enough sources have been examined to determine any preferential range or bearing and this will be performed in the future. Of the approximately 20 sources examined, no obviously active areas were found.

SOURCE DIRECTIVITY

To aid in modelling the source characteristics, a technique (involving several steps or programs) was developed to determine the vertical directivity of the transient sources. The directivity of a given transient is found in the following manner:

a) The eigenrays for all hydrophones in the vertical array for the ranges specified in the section "Source Localization" are first calculated and a table of the arrival times, path lengths and source angles for all these hydrophones and ranges is computed and stored. Note this need only be performed once and the lookup table can then be used for a specific hydrophone and source range. To compute the path lengths, the routine "Plot Rays" in the SONAR model was modified. This new version of "Plot Rays" is identical to that described in the SONAR manuals except that instead of plotting rays at user specified angles, it calculates the ray path lengths for rays at the angles listed in the eigenray file and prints these path lengths into the eigenray file. It may be used by running "OA$CENTRAL:[SONAR.GREENING.PATH]CMP_LEN" instead of "SONAR". The documentation, data files, command files and programs required, along with an example of how to produce the arrival times, path lengths and source angle files for specific environmental conditions are available in the directories:

"OA$CENTRAL:[SONAR.GREENING.DIRECTIVITY]" and

"OA$CENTRAL:[SONAR.GREENING.TIME]"

b)   A specific transient is then identified as outlined in "Source Detection and Description" and the direct arrival and bottom reflection are individually removed from the data so the power spectra of these arrivals can be obtained. Note that an independent section of data is removed for each hydrophone to ensure that other arrivals which overlap in time across the array are not included.   The bottom-surface reflection and further multiples cannot be used because reflection from the ice is highly incoherent.   Only those bottom reflections with grazing angles below critical angle (for which the coherent reflection coefficient is assumed to be unity) can be used.

c)   The power spectra of these arrivals are then obtained. This was done by zero padding all arrivals to 256 data points and using a 32 point FFT with 24 point overlap. Note that due to the large SNR of the transients used, it was not necessary to model and remove the background noise when calculating the power spectra.

d)   The source range is then determined as outlined in "Source Localization".

e)   The source directivity is then calculated and plotted as a function of source angle determined in a). The source directivity at a given angle is the sum of the observed power and the propagation loss where the propagation loss is calculated assuming spherical spreading over the path length calculated in a).

Figures 15-18 show typical plots of source directivity for four transients at increasing ranges (60m, 420m, 530m, and 1400m). Note that only the direct arrival is

used with the closer three transients while the 1400m range transient shows the directivity from the direct arrival and the bottom reflection. The reflection coefficient for the bottom at these shallow grazing angles (less than 30 degrees) was assumed to be unity and thus the true source energy measured from the bottom reflection may be higher (if the reflection coefficient was less than unity) but cannot be lower. Transients at ranges greater than 2000m were not used to determine source directivity because of overlap of the direct arrival and bottom reflection on the deeper hydrophones. From these figures it is seen that the source directivity has a gain of approximately 15dB from 5 to 15 degrees from horizontal at 50 or 100Hz and a further gain of 10dB from 15 to 90 degrees. At higher frequency, 150Hz, this gain increased to 20dB from 5 to 15 degrees and 15dB from 15 to 90 degrees. Presently, the directivity of about 15 transients has been determined and more transients should be examined to obtain confidence in these results and determine if the source directivity varies as a function of some other source characteristic.

BOTTOM REFLECTION

Along with the data collection of arctic noise, several recordings using artificial sources (light bulbs) were also made to aid in determining propagation characteristics such as sub-bottom structure and reflection coefficients. These artificial sources were used at both 150m and 1431m ranges and recorded on hydrophones at depths of 18m, 54m, 102m, 150m, 198m, 246m and 294m. The light bulbs were weighted and dropped into the water and the resulting implosion sampled at 8192Hz and low pass filtered at approximately 2000Hz. The exact ranges and source depths were determined by matching arrival times as previously shown for finding the range of transient noise. Figures 19-22 show the array output for light bulb sources at two

different depths for both the 150m and 1431m ranges. Note that the direct arrival has saturated hydrophone number 5 for the 210m depth source at 150m range (figure 20).

Because these sources are omni-directional, the measured difference in power between the direct arrival and bottom reflection, after correction for propagation loss, will be the bottom reflection coefficient. Then, by measuring the reflection coefficient for several frequencies and grazing angles, the bottom characteristics (sub-bottom structure, density and sound speed) can in principle be determined by an inverse fit to a multi-layered model as outlined in Brekhovskikh. The fitted bottom characteristics can then be used to estimate the reflection coefficient for other frequencies and grazing angles, such as those for the transient ice noise, thus allowing bottom reflections to be used in determining source directivity.

To produce a first estimate of the bottom characteristics, a 6cm long core of bottom sediment was obtained and used in conjunction with refraction measurements The core consisted of quartz sand with a compressional sound speed of 1980m/sec which is often found to be up to a few meters deep overlying a thick layer (up to 100m) of hard sediment with a sound speed of 200m/sec to 500m/sec higher than that of the upper unconsolidated sediment layer. The upper layer often consists of several smaller layers of sand, mud, etc., with sound speed differences of 20m/sec to 100m/sec. The densities of these sediment layers is typically 1.6gm/cc to 2.1gm/cc with the higher densities at greater depths.

For a bottom sound speed of 1980m/sec and density of 1.6gm/cc, the critical angle is approximately 50 degrees and thus, any reflection with grazing angles below 50 degrees will have perfect internal reflection. This is shown in figure 23 where it is seen that the energy of the direct arrival and bottom reflection are nearly equal for all

except the high frequencies which contain little energy. Thus, none of the 1431m range sources, for which the bottom grazing angles are 20 to 30 degrees, are useful for determining bottom characteristics (other than surface roughness) and the 150m range sources have to be used.

In examining the spectra for the 150m range sources, an unexpectedly high energy content was observed in the direct arrival below 200Hz as shown in figure 24. The spectra for this type of source should be a single broad band peak with a bandwidth of approximately 1000Hz to 1500Hz dependent on the depth at which implosion occurred. The high energy observed at low frequency occurs because the direct arrival saturated the hydrophones for the 150m range shots as shown in figure 25. (The drop to zero voltage of the 150m range source at about 0.022sec is due to zero padding for performing the FFT.) It is unclear how this saturation effects the entire spectrum and a comparison of the spectra for a distant and close source at the same depth is shown in figure 26. Because of the uncertainty in the power spectra for the close range direct arrival, measurements of the reflection coefficients could not be made accurately and the bottom characteristics were not completely determined.

Although the exact bottom characteristics were not found, evidence of two sub-bottom layers at approximately 3m and 15m depth were found as shown in figures 27 and 28 respectively. These depths were calculated assuming a constant bottom sound speed of 2000m/sec. Reflection from the 3m deep sub-bottom layer was consistently seen in all 150m range sources while the weaker 15m depth reflection was not visible on several sources. A 3m deep sub-bottom layer is also consistent with the periodicity in the measured bottom reflection power spectra (figure 23) using the multi-layered model from Brekhovskikh.

A final observation made from the light bulb sources is evidence of either channelling occurring in the water column or focussing occurring due to bottom roughness. This can be seen because the bottom reflection (for which the propagation path is longer and reflection from the bottom has occurred) occasionally had higher power than the direct arrival as shown in figure 29. It is assumed that this is probably due to channelling which can occur with a sound speed gradient present in the water. Focussing due to bottom roughness is not expected because of the near reproduction of the direct arrival by the bottom reflection (as shown in figure 30) indicating an acoustically flat bottom for these frequencies. It is unknown how much of an effect this channelling will have on the calculated propagation losses used to determine source directivity and this may have to be accounted for.

CONCLUSIONS

A simple transient detection system based on the peak height versus the average peak height over a long time series was used to detect and extract transient sources from the background noise. This simple source detection technique found an average and median of approximately 4 and 2 transients respectively per 2 minute sample of data. Multichannel displays of these transients then revealed several characteristics of the sources and propagation such as definite evidence of source directivity (i.e. the source does not appear to be a monopole); a time scale over which a transient increases the noise level in the order of 0.1 to 0.4 seconds for a specific arrival and up to 1 second when including multiple arrivals; and also, the existence of arrivals caused by the leakage of energy from the symmetric plate wave in the ice.

A method of localizing the source (finding the range and bearing) was developed using the ray tracing model SONAR from Ocean Acoustics. This was done to determine if the sources are randomly distributed or are concentrated in specific areas. To date, not enough sources have been localized to obtain any conclusions and this should be performed in the future.

A technique for determining the vertical directivity of these transients was then developed to aid in modelling the source characteristics. Several sources were examined and found to have a loss of approximately 15dB from 5 to 15 degrees from horizontal at 50 or 100Hz and a further loss of 10dB from 15 to 90 degrees. At higher frequency, 150Hz, this loss increased to 20dB from 5 to 15 degrees and 15dB from 15 to 90 degrees. More transients should be examined to obtain confidence in these results and determine if the source directivity varies as a function of some source characteristic other than frequency.

Recordings of artificial sources (i.e. light bulbs) were examined to determine bottom characteristics such as sub-bottom structure and reflection coefficients. These artificial sources clearly indicated sub-bottom layers at about 3m and 15m depths. Although an exact model of the reflection coefficients for all frequencies and grazing angles could not be determined, it was seen that the coherent reflection coefficient for grazing angles below the critical angle (roughly 50 degrees) is approximately 1.

FIGURES 1 - 30

Array Configurations

a) Configuration #1
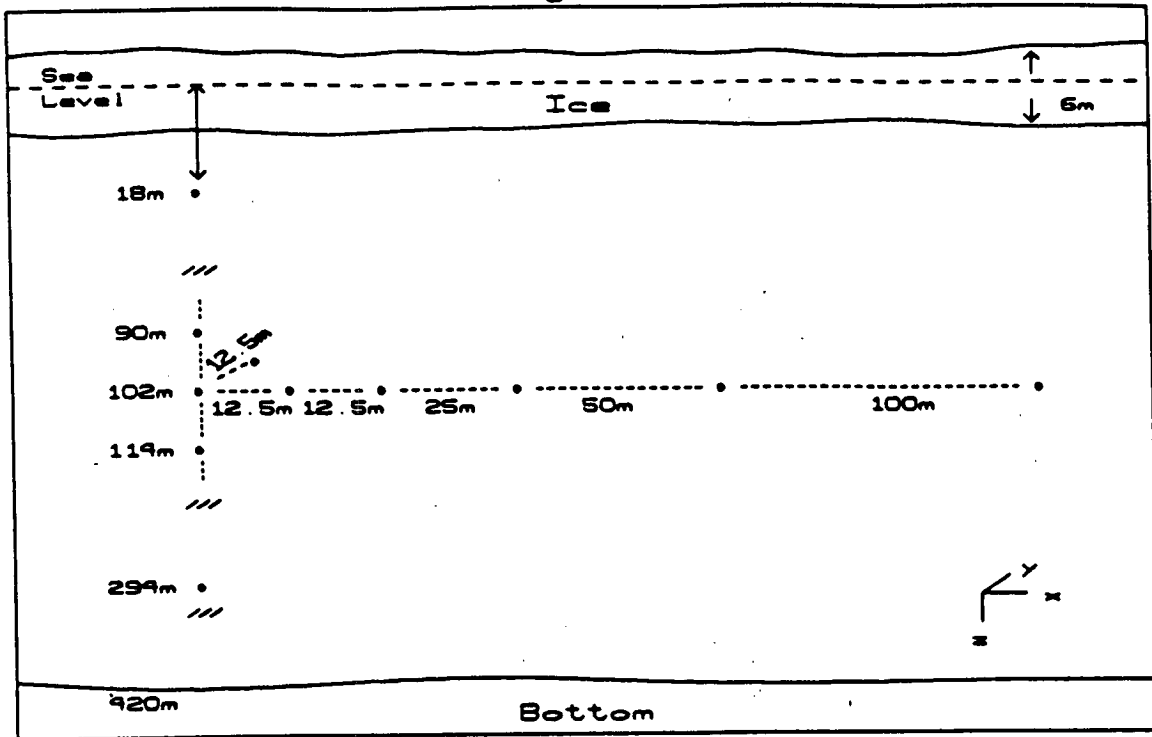
b) Configuration #2
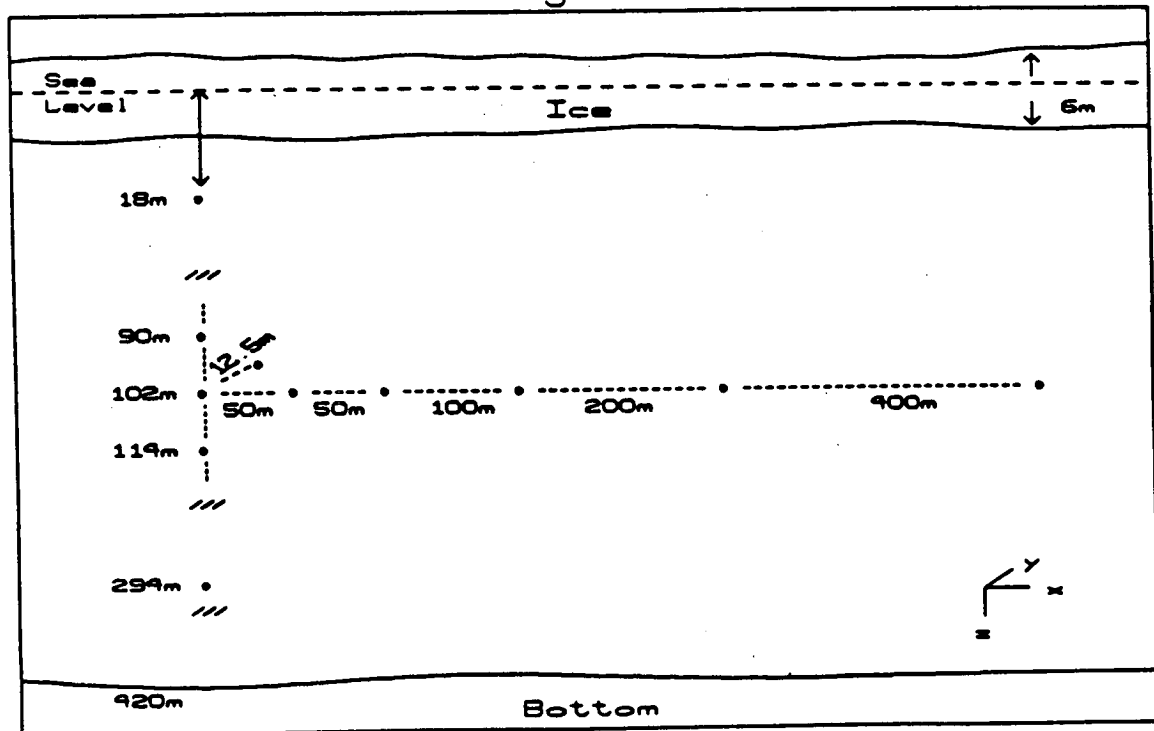
Figure 1

Figure 2. Source Range = 60 m
Peak Height to Average Ratio = 43

D – Direct Arrival
B – Bottom Reflection
BS – Bottom Surface Reflection
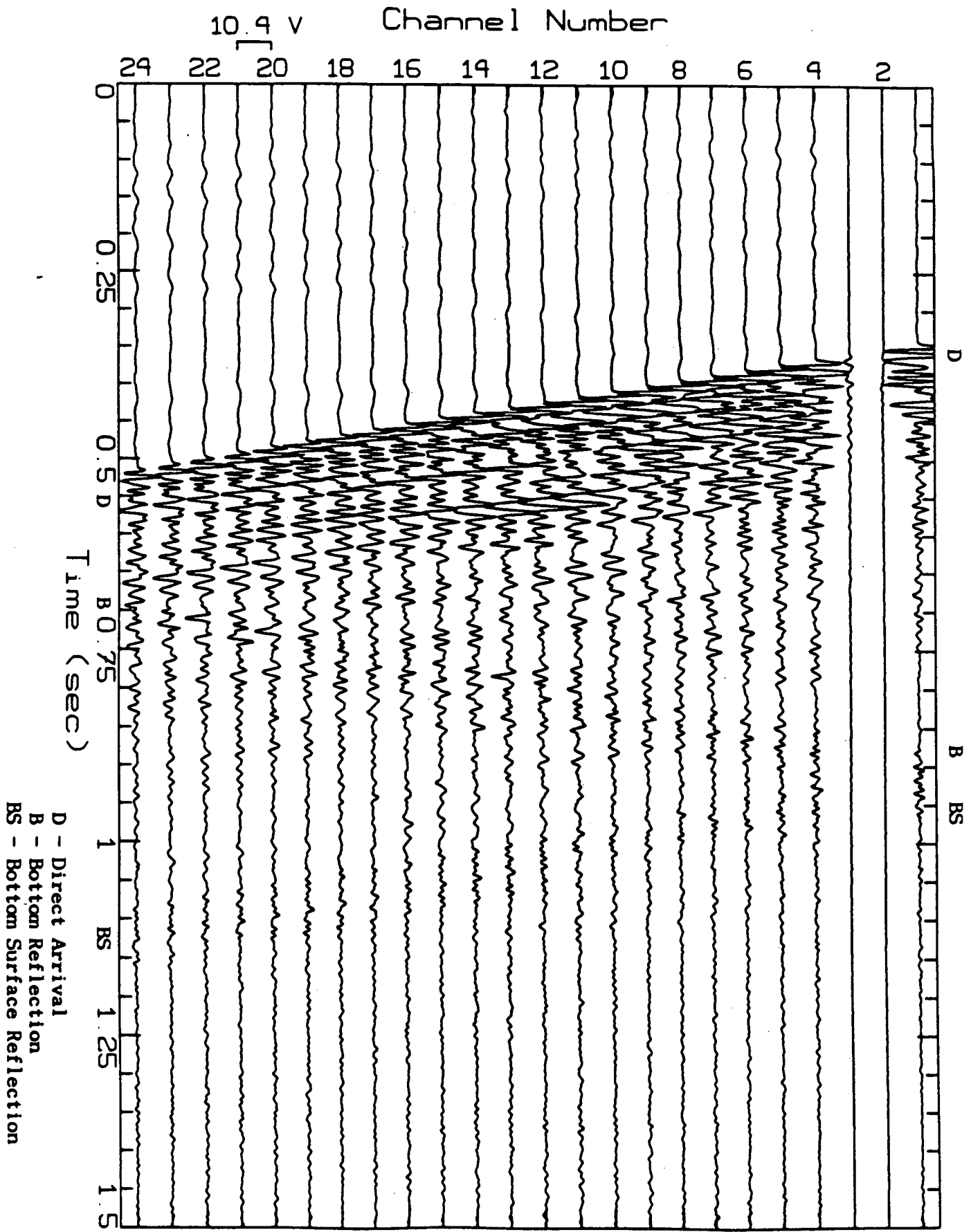
Figure 3. Source Range = 480 m
Peak Height to Average Ratio = 18
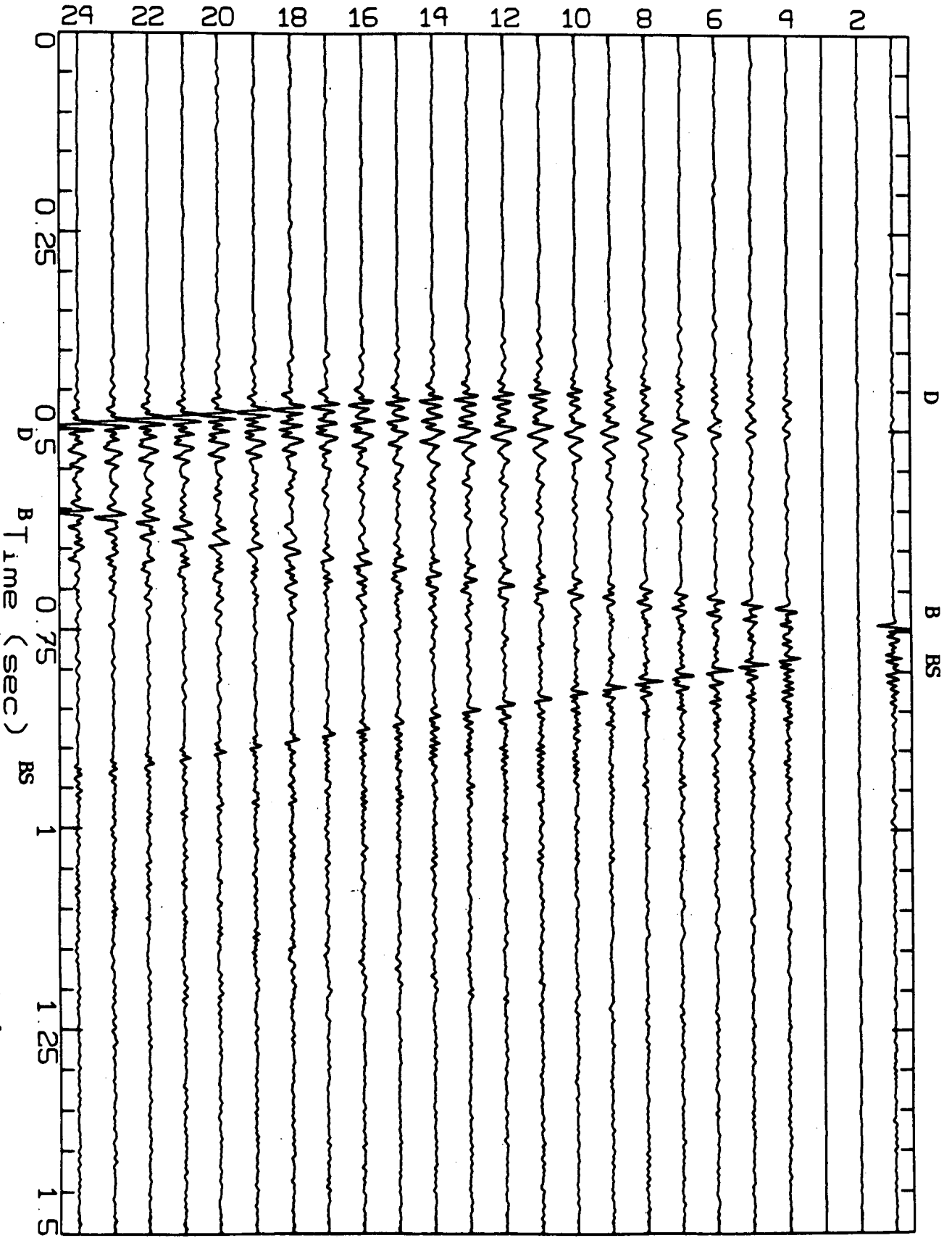
D – Direct Arrival
B – Bottom Reflection
BS – Bottom Surface Reflection

Figure 4. Source Range = 470 m
Peak Height to Average Ratio = 9
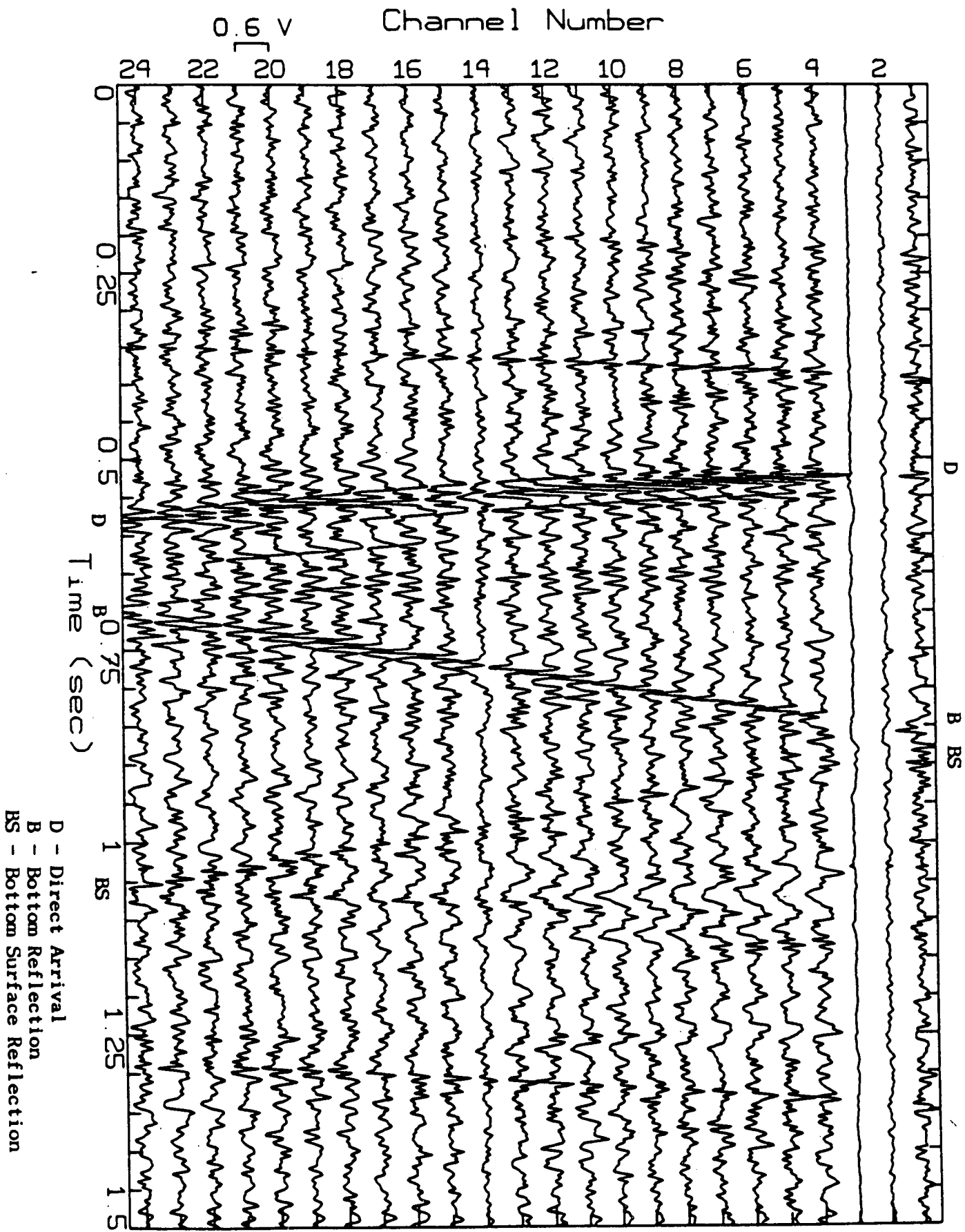
D - Direct Arrival
B - Bottom Reflection
BS - Bottom Surface Reflection

Figure 5. Source Range = 3150 m
Peak Height to Average Ratio = 26
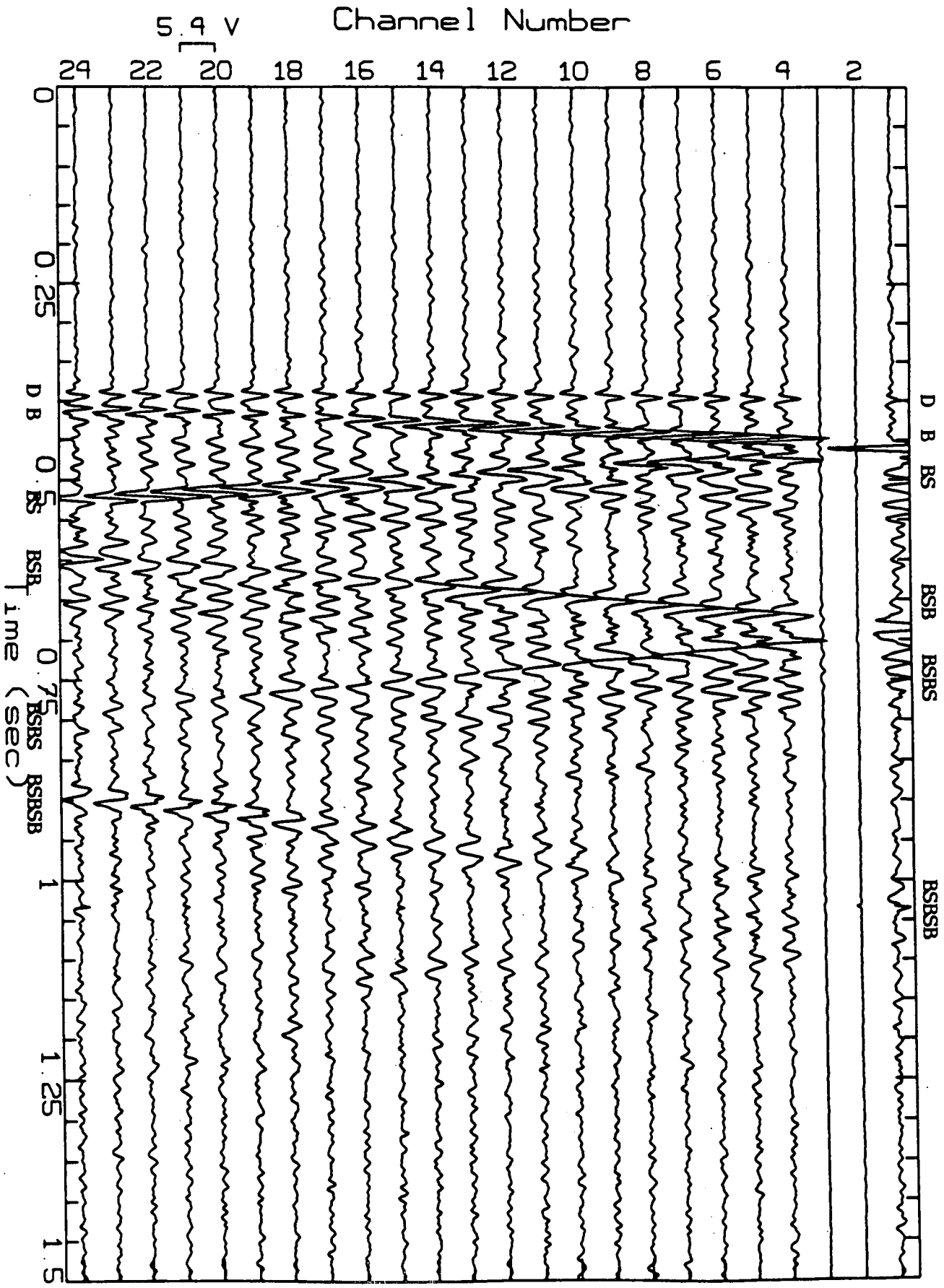
Channel Number

5.4 V

Time (sec)

D — Direct Arrival
B — Bottom Reflection
BS — Bottom Surface Reflection

Figure 6. Source Range = 3500 m
Peak Height to Average Ratio = 14

D – Direct Arrival
B – Bottom Reflection
BS – Bottom Surface Reflection
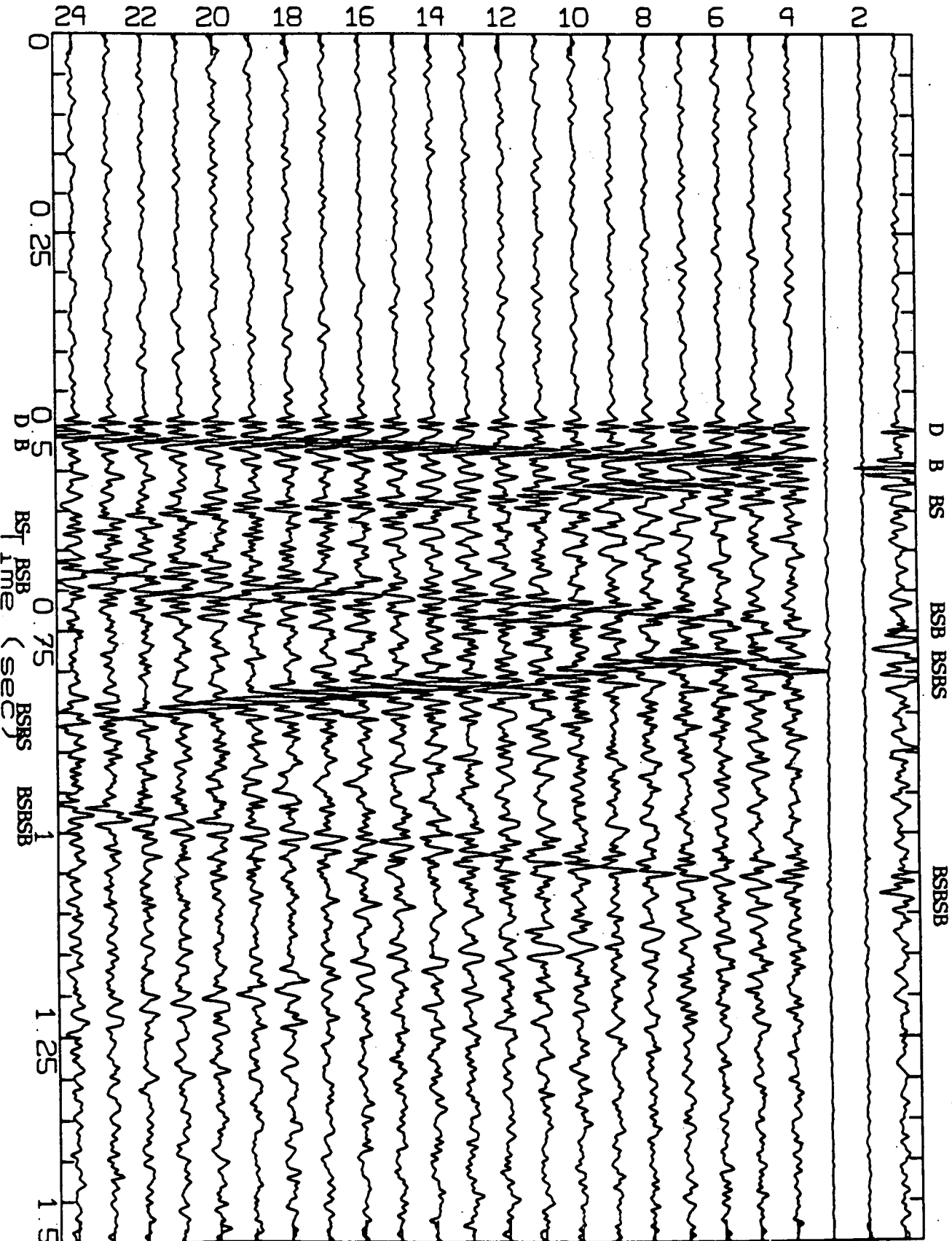
Figure 7. Source Range = 3000 m
Peak Height to Average Ratio = 7

Channel Number

0.7 V

D — Direct Arrival
B — Bottom Reflection
BS — Bottom Surface Reflection
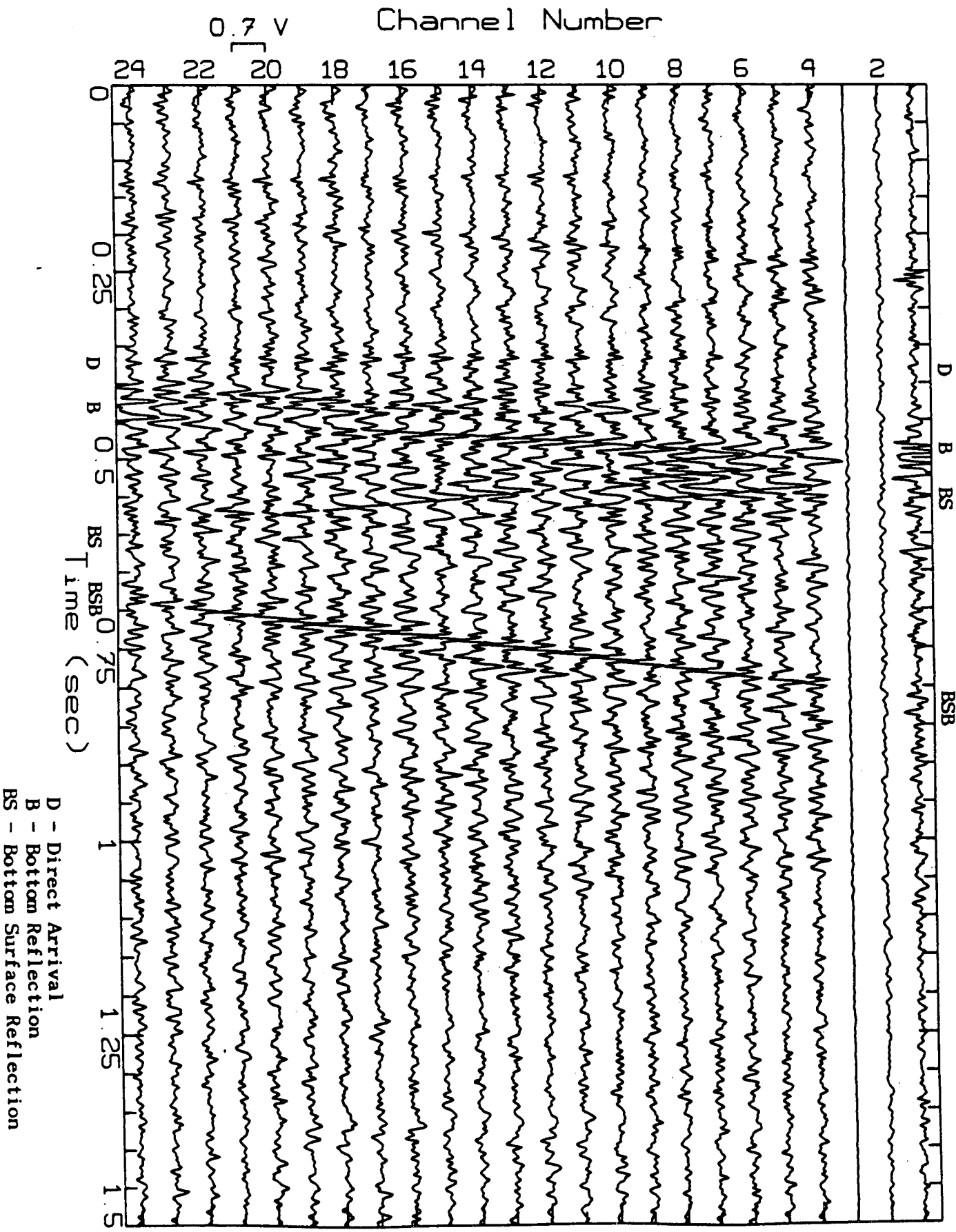
Figure 8. Source Range = 400 m With Precursor.

P - Precursor
D - Direct Arrival
B - Bottom Reflection
BS - Bottom Surface Reflection
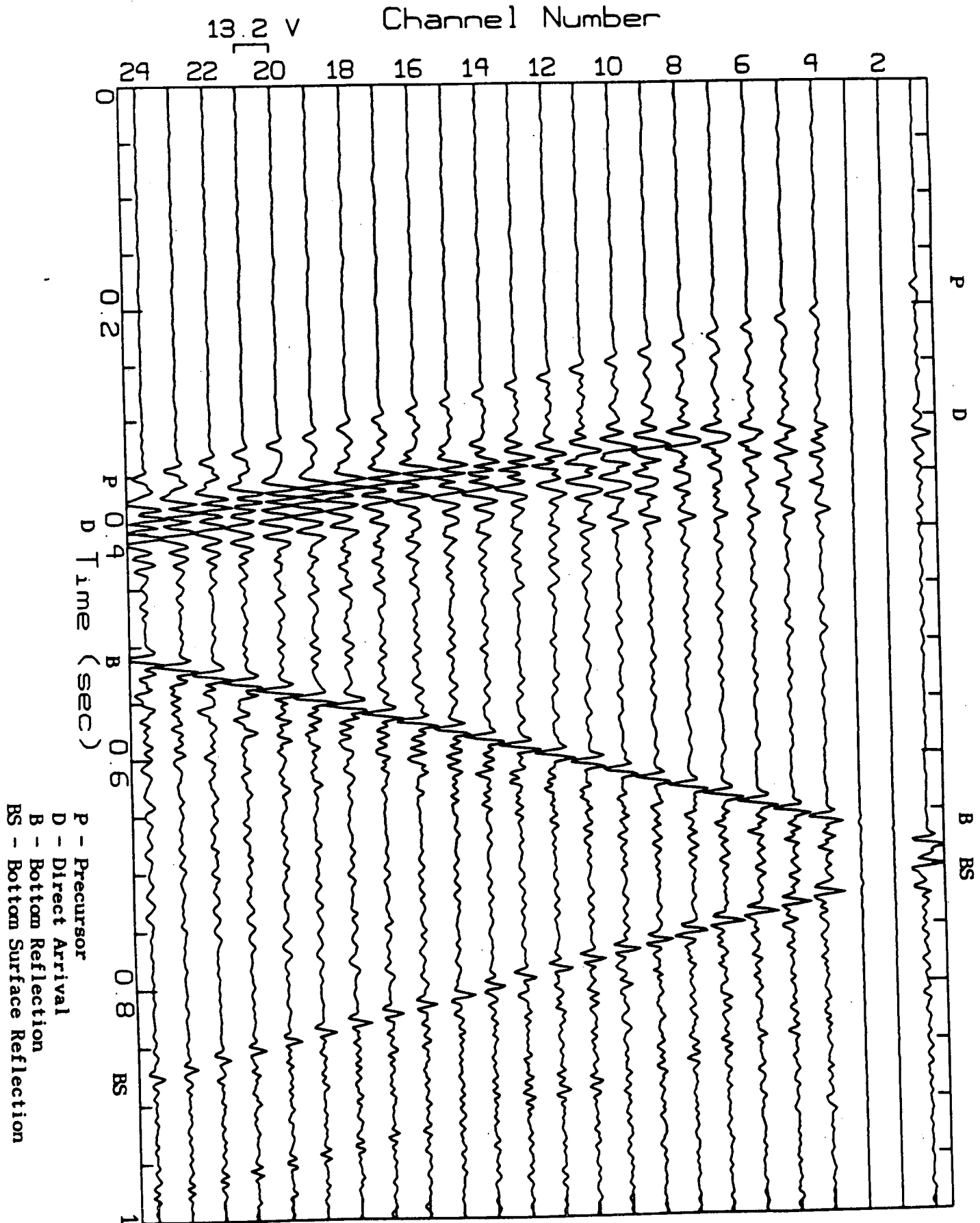
Sound Speed Profile
Measured (solid)   Used (dash)
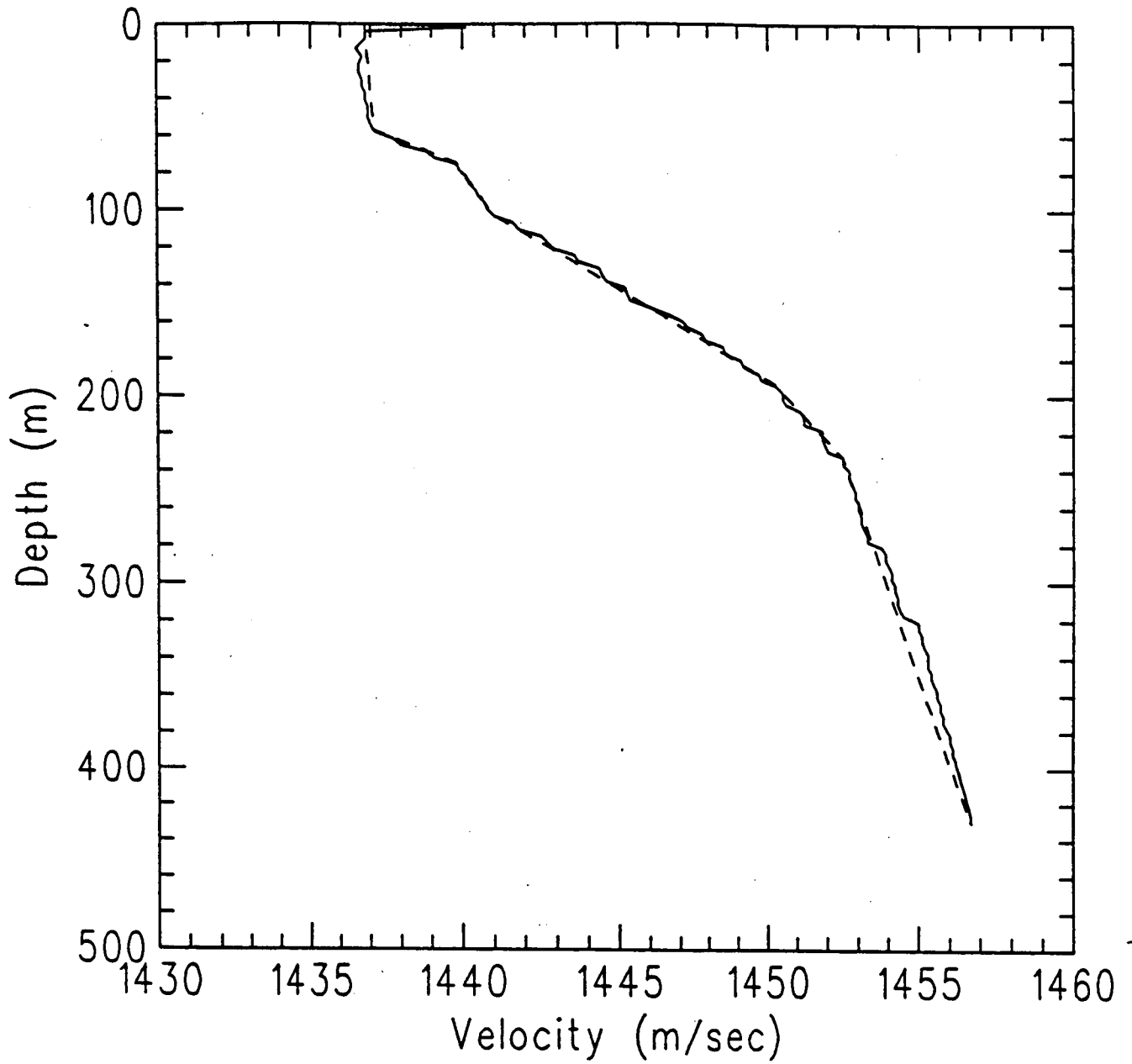
Figure 9.

MULTIPATH EIGENRAY MODEL:
ACOUSTIC EIGENRAYS JOINING A SOURCE AT
(0m, 0m) TO RECEIVER AT (5000m, 294m)
IN WATER OF 430m DEPTH
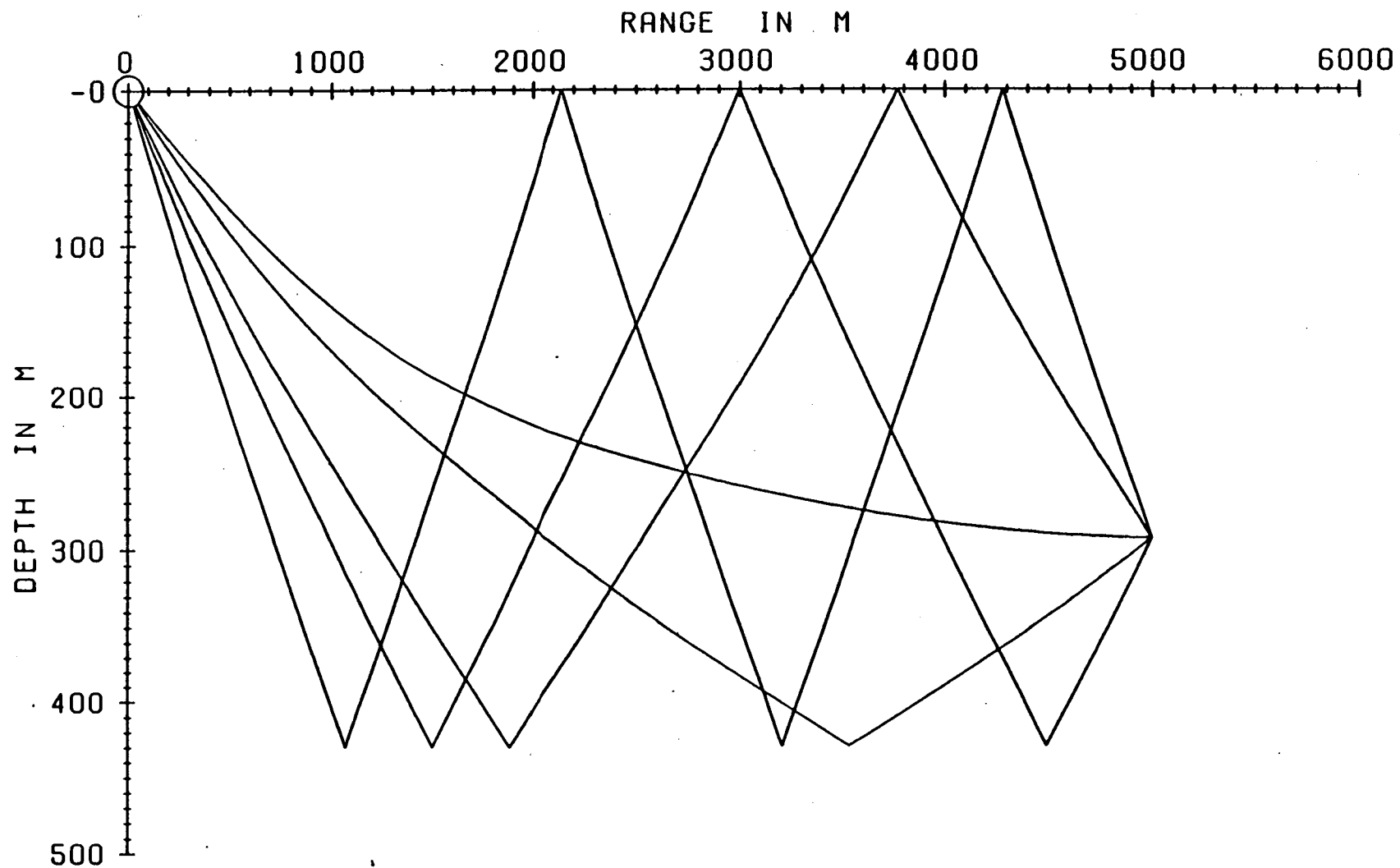
Figure 10.

Figure 11. Source Range = 510 m
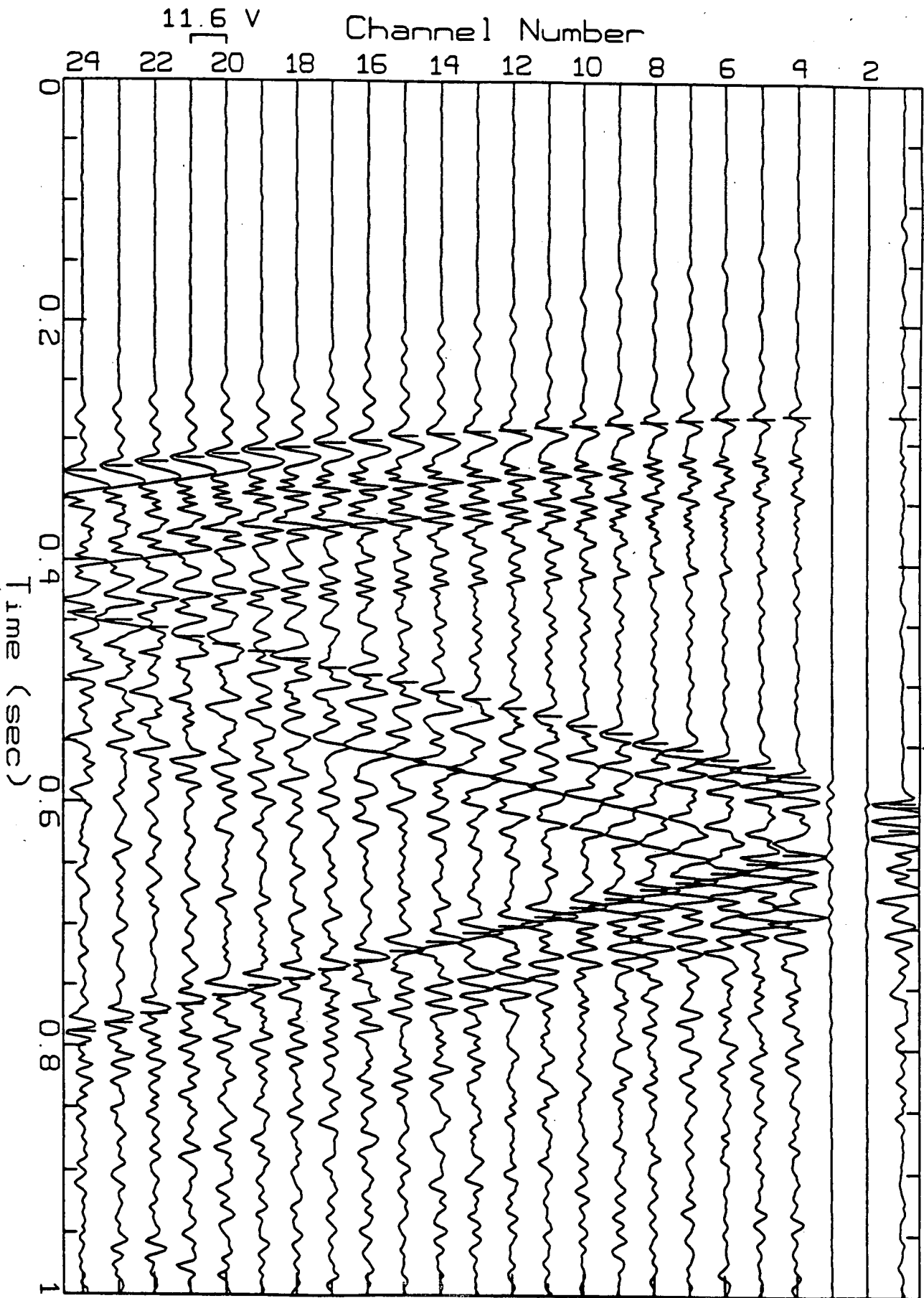
Figure 12. Source Range = 3900 m

Figure 13. Source Bearing = 240°

Figure 14. Source Bearing = 153°
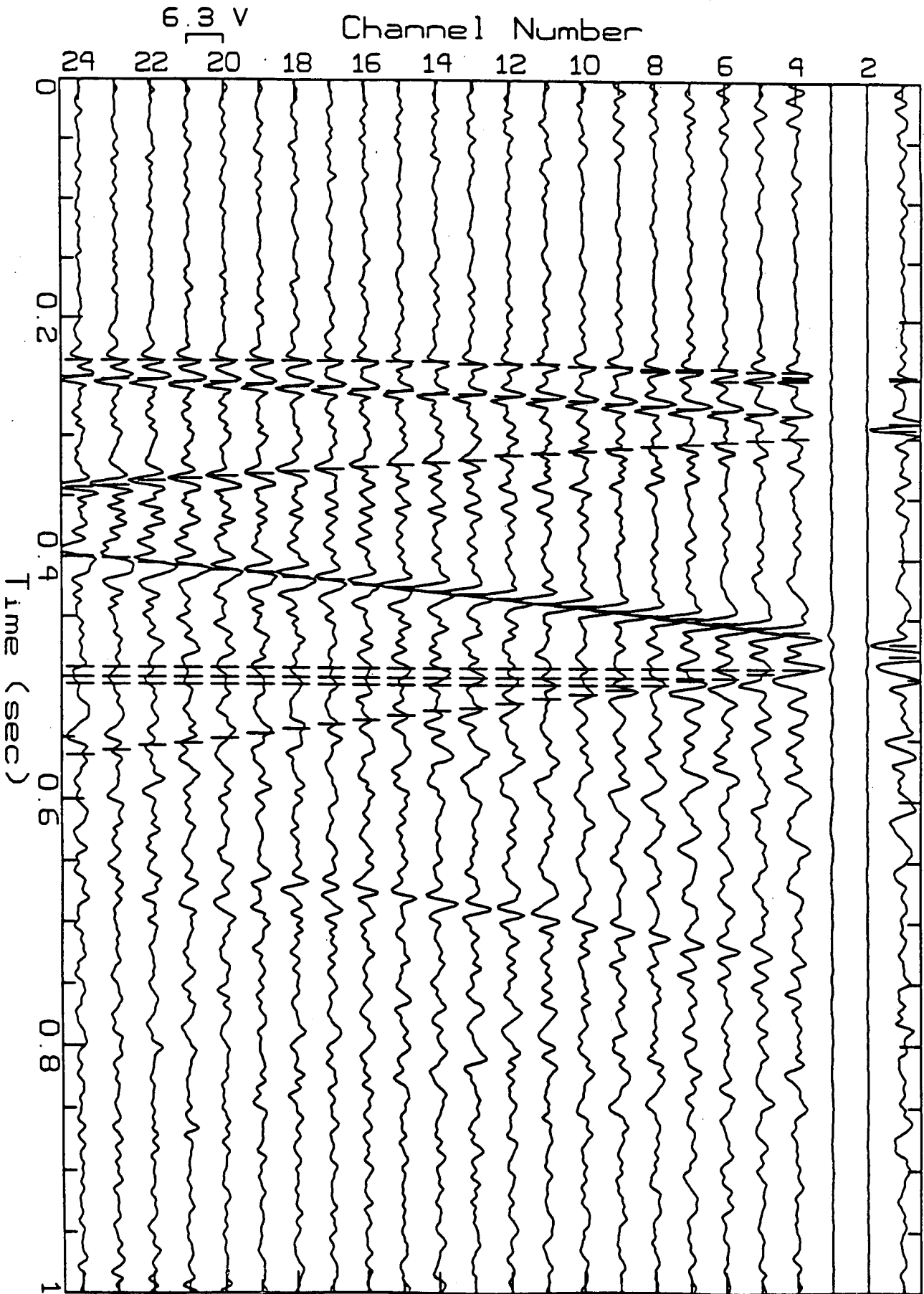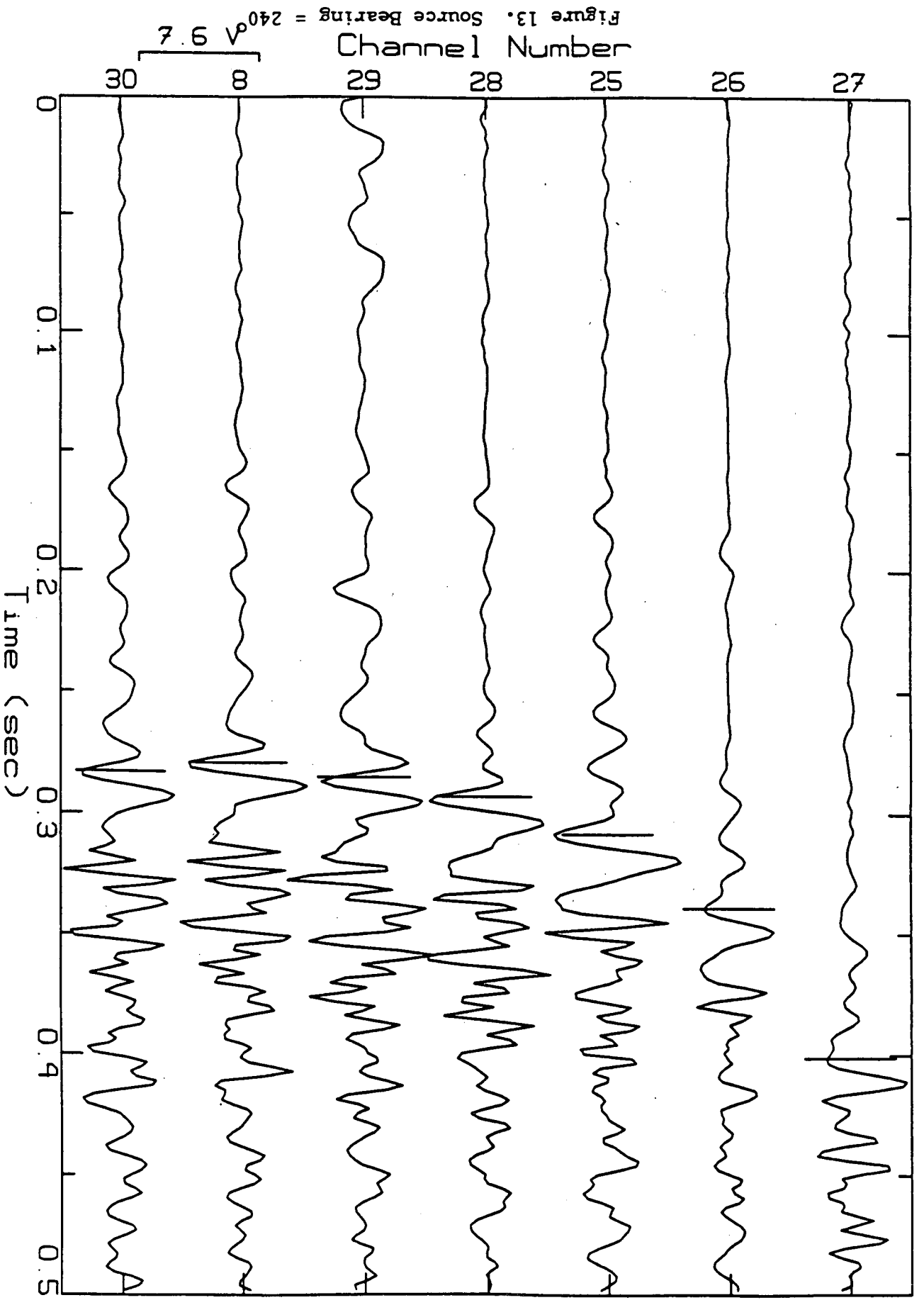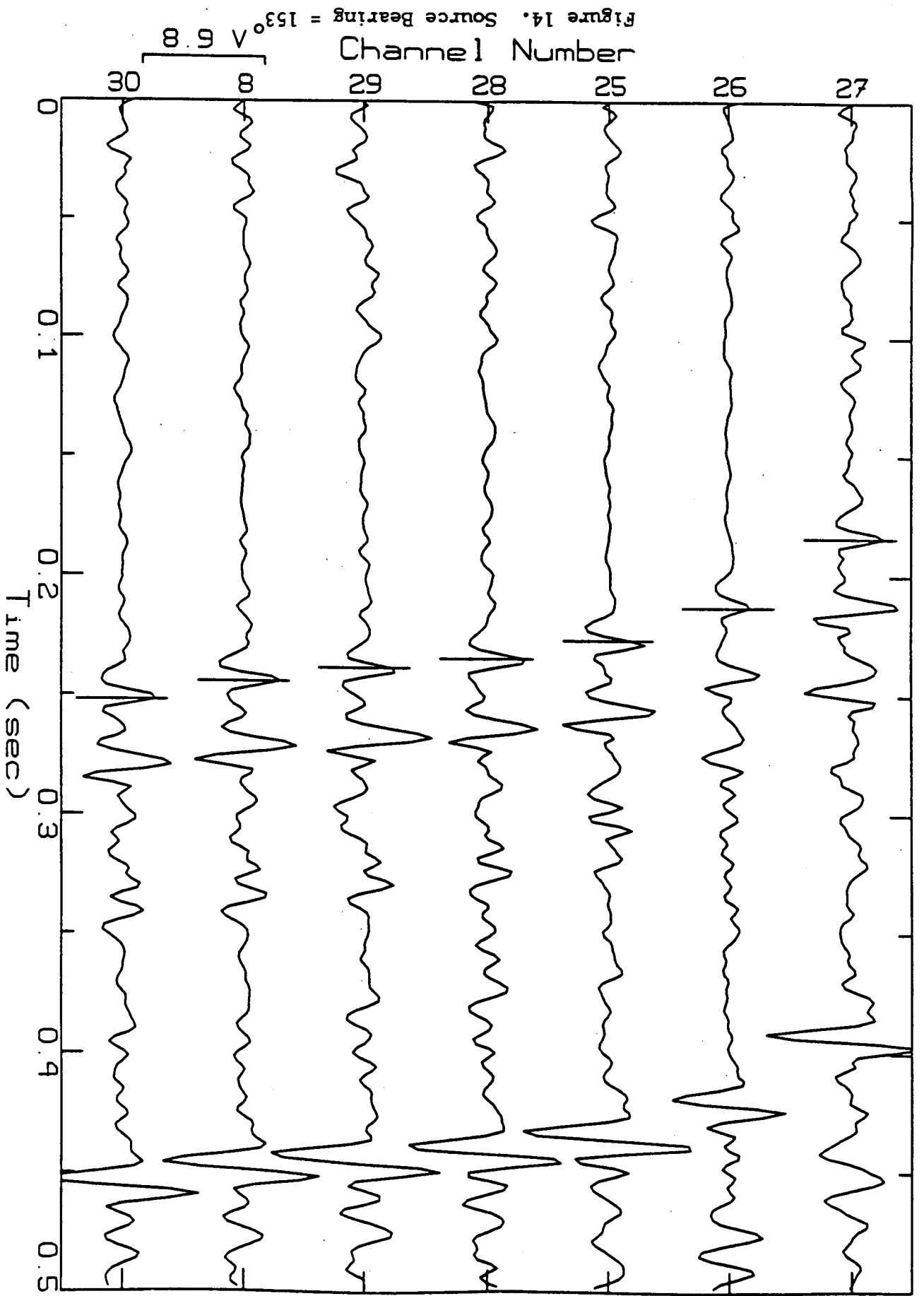
Source Directivity
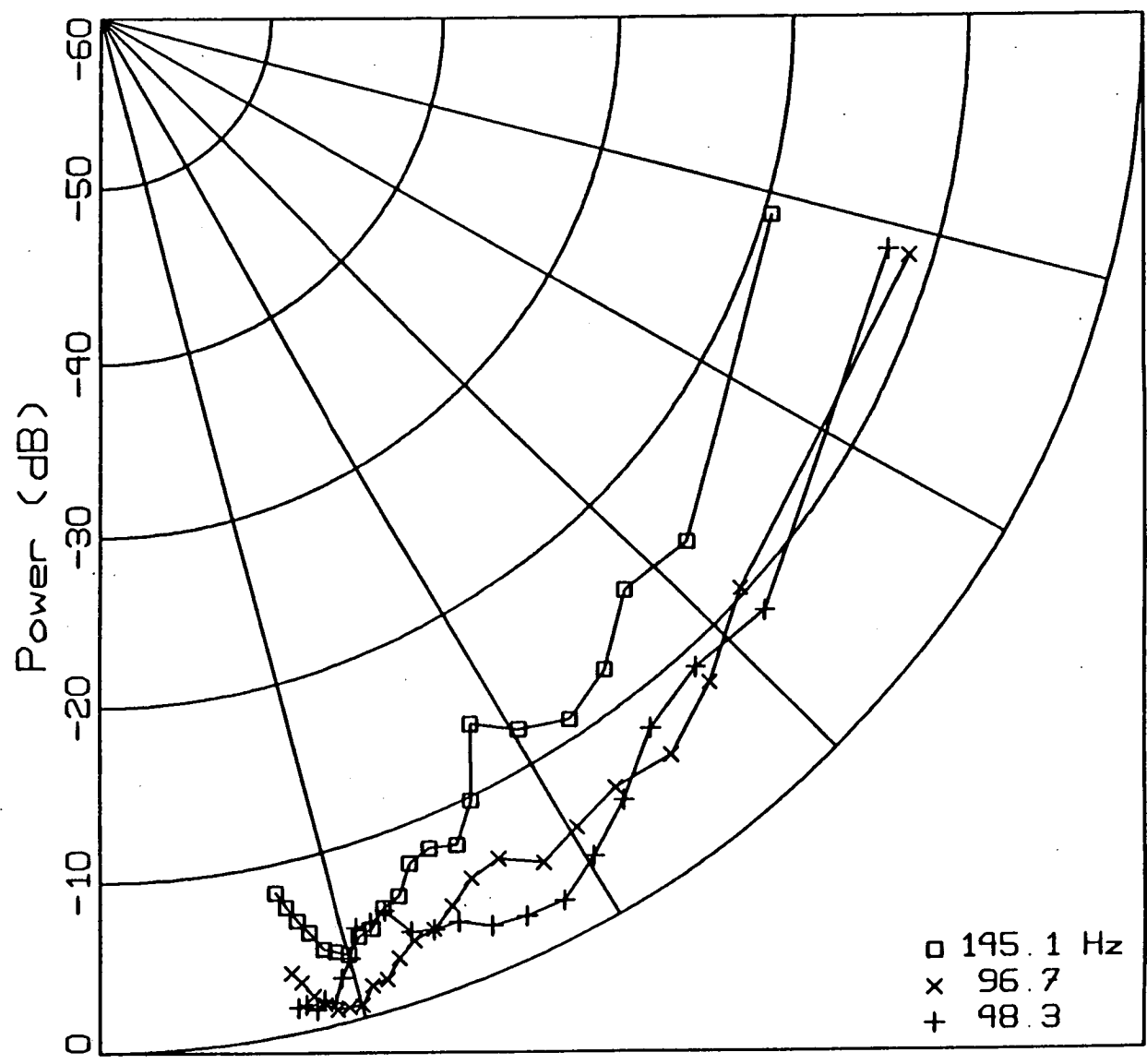
Figure 15. Source Range = 60 m

Source Directivity
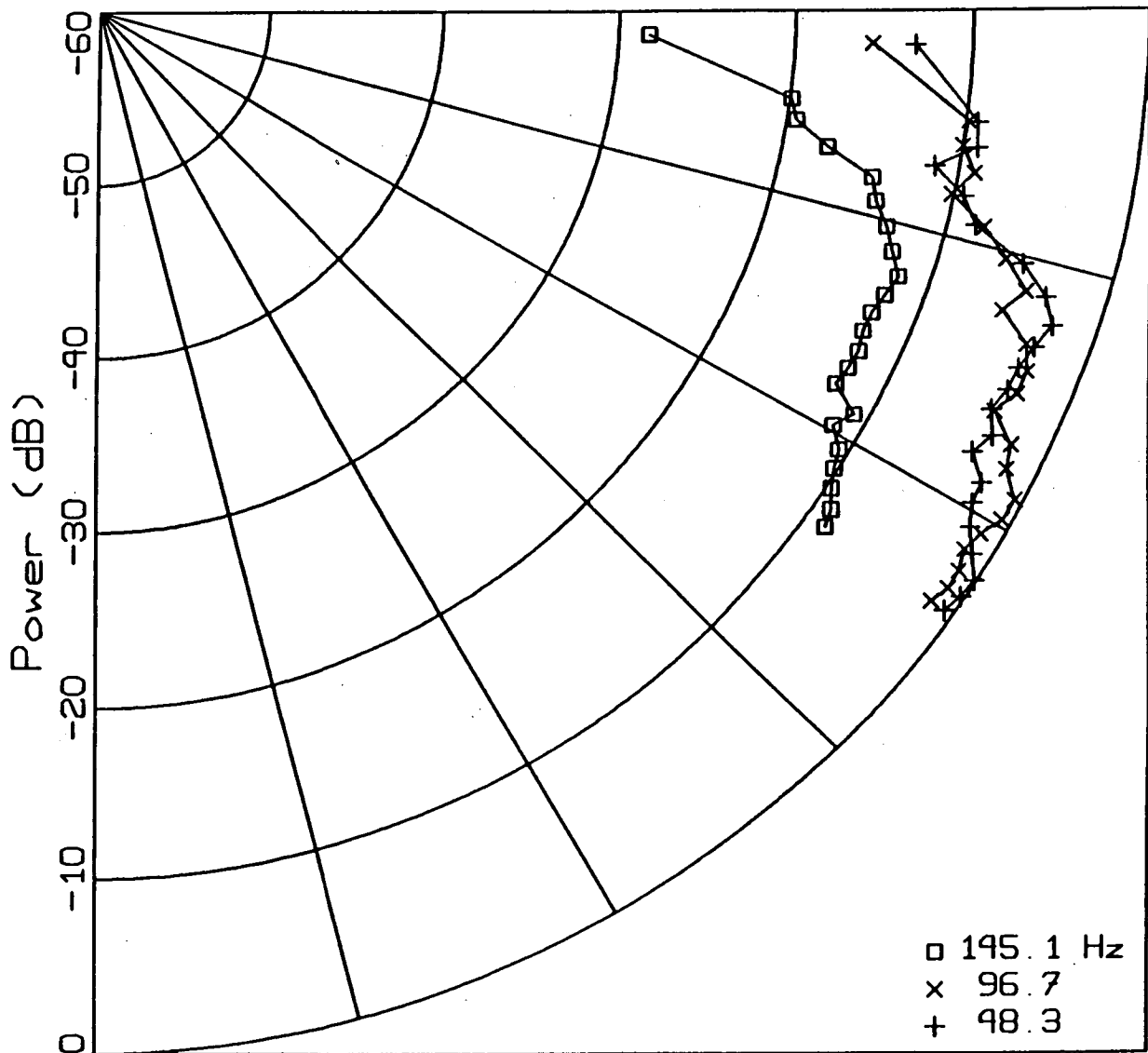
Figure 16. Source Range = 420 m

Source Directivity
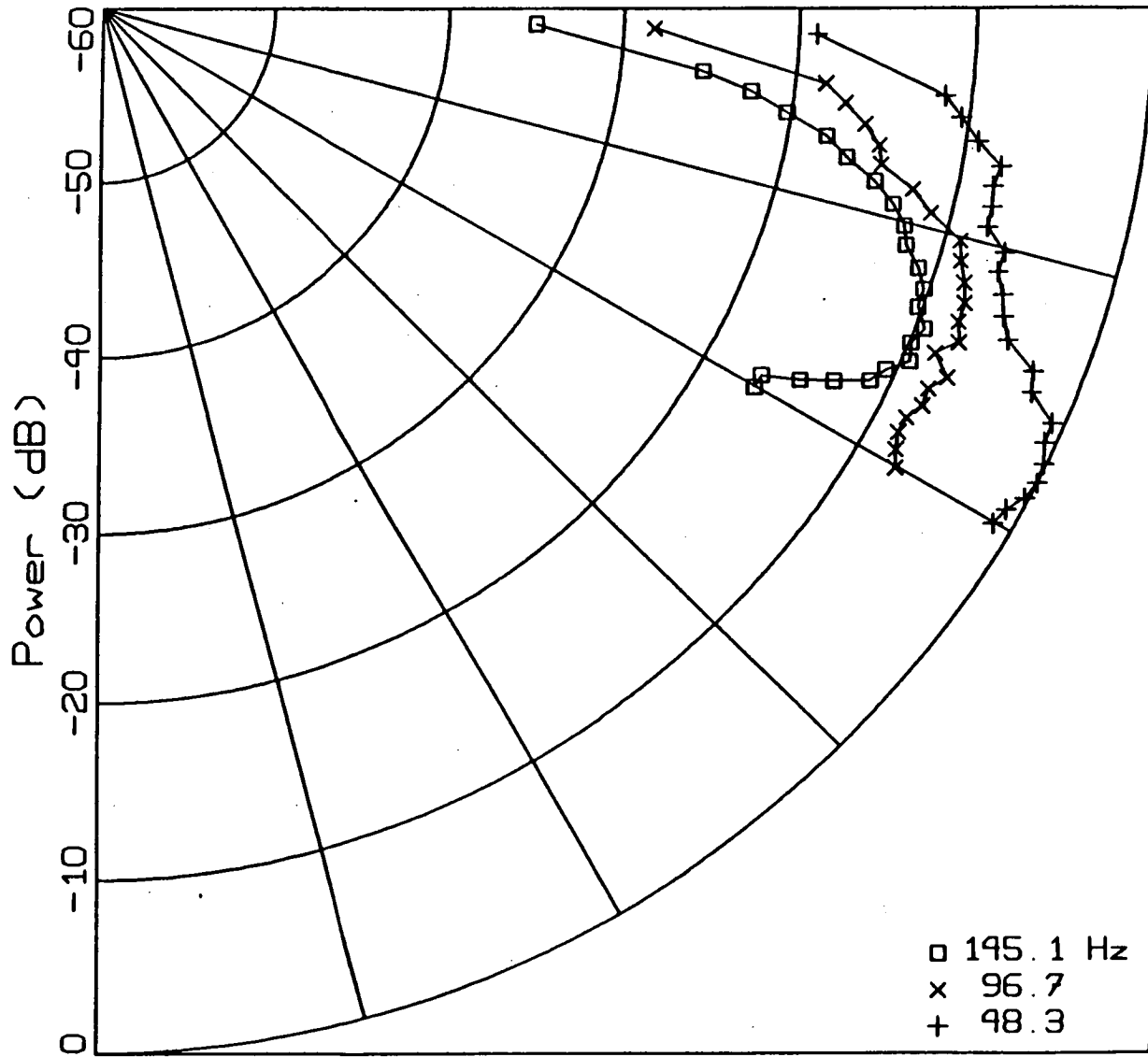
Figure 17. Source Range = 530 m

□ 145.1 Hz
× 96.7
+ 48.3

Power (dB)

Source Directivity
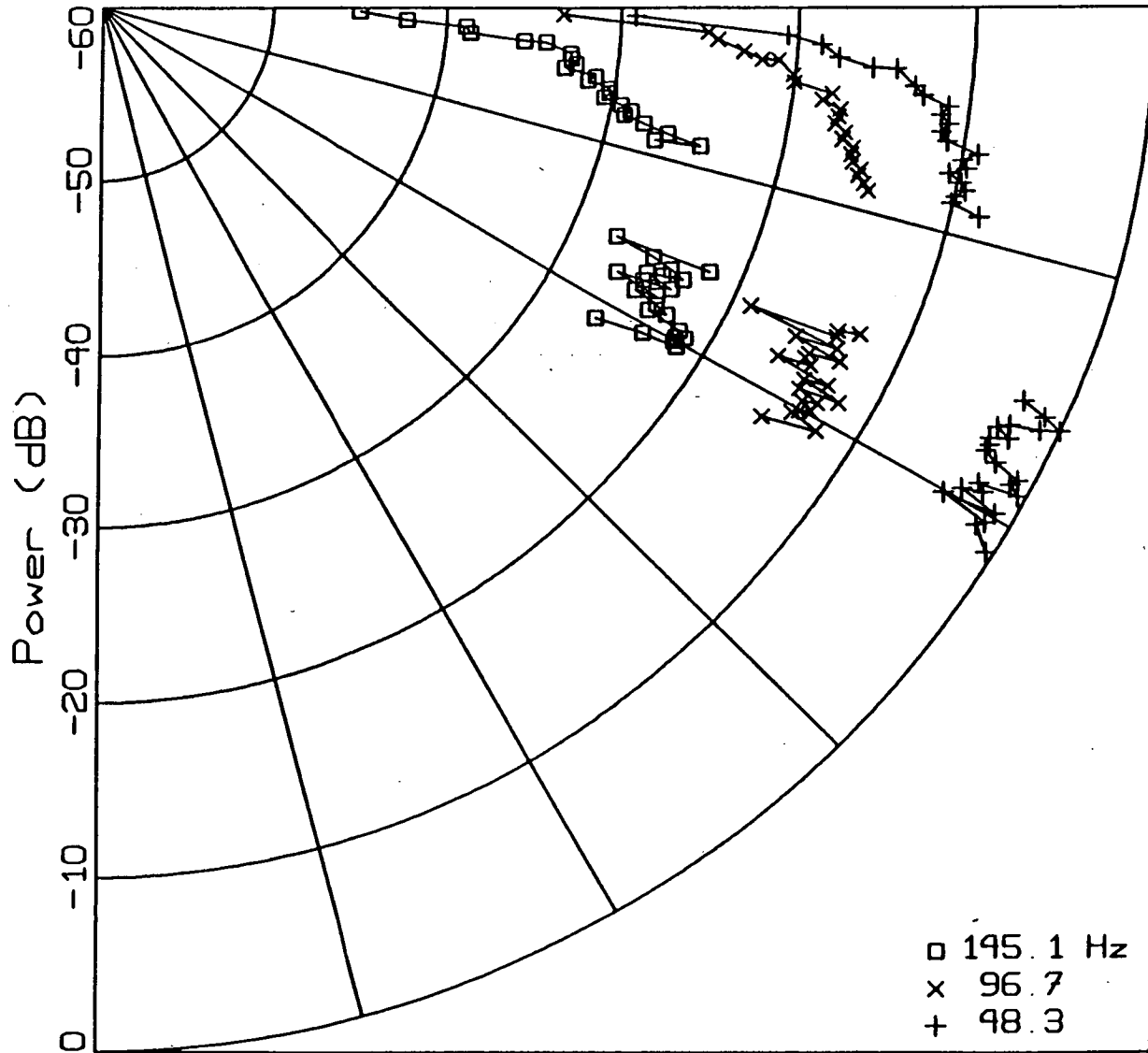
Figure 18. Source Range = 1400 m

□ 145.1 Hz
× 96.7
+ 48.3

Power (dB)

Figure 19. Source Range = 150 m, Source Depth = 110 m
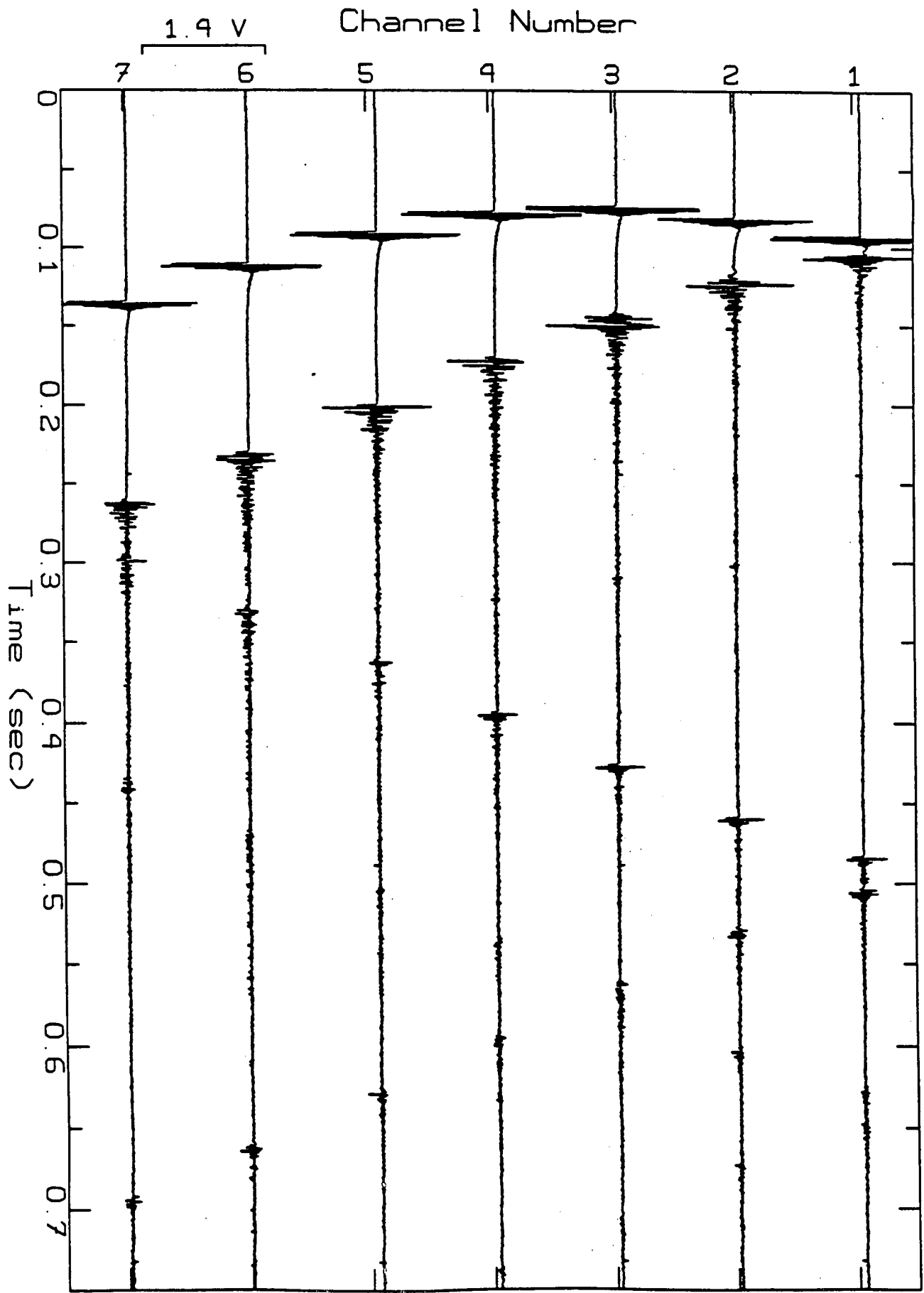
Figure 20. Source Range = 150 m
Source Depth = 210 m
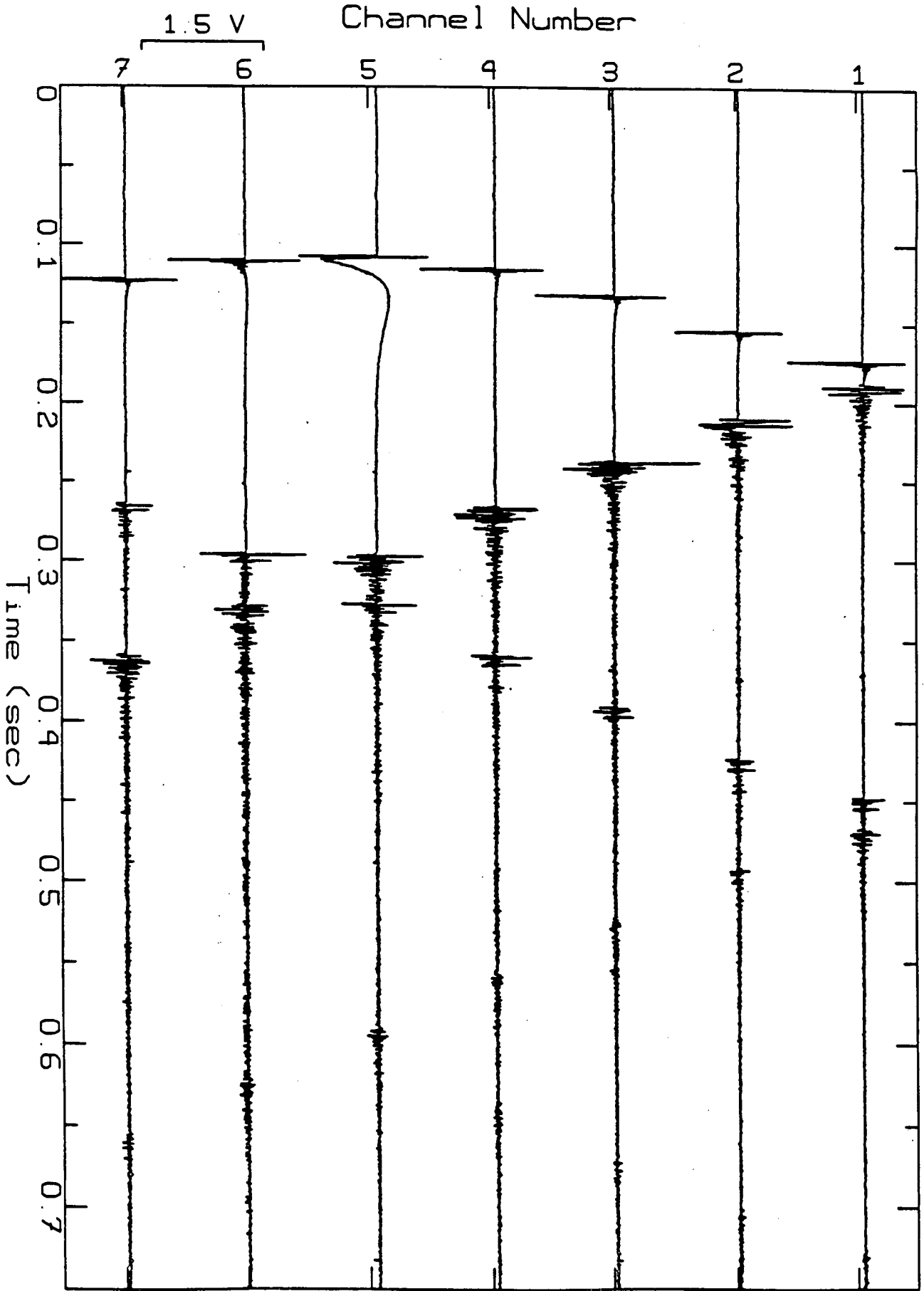
Figure 21. Source Range = 1431 m
Source Depth = 116 m
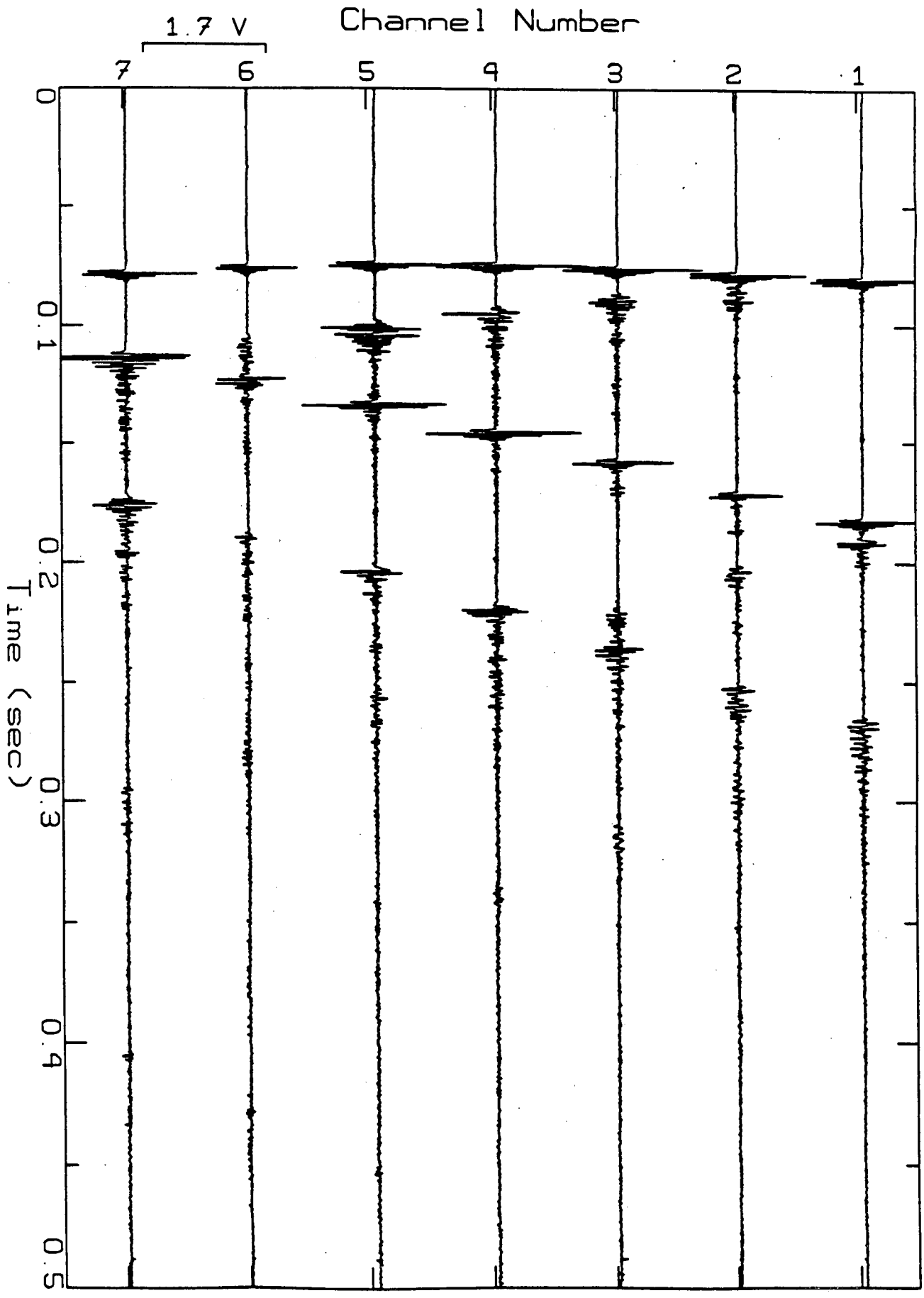
Figure 22. Source Range = 1431 m
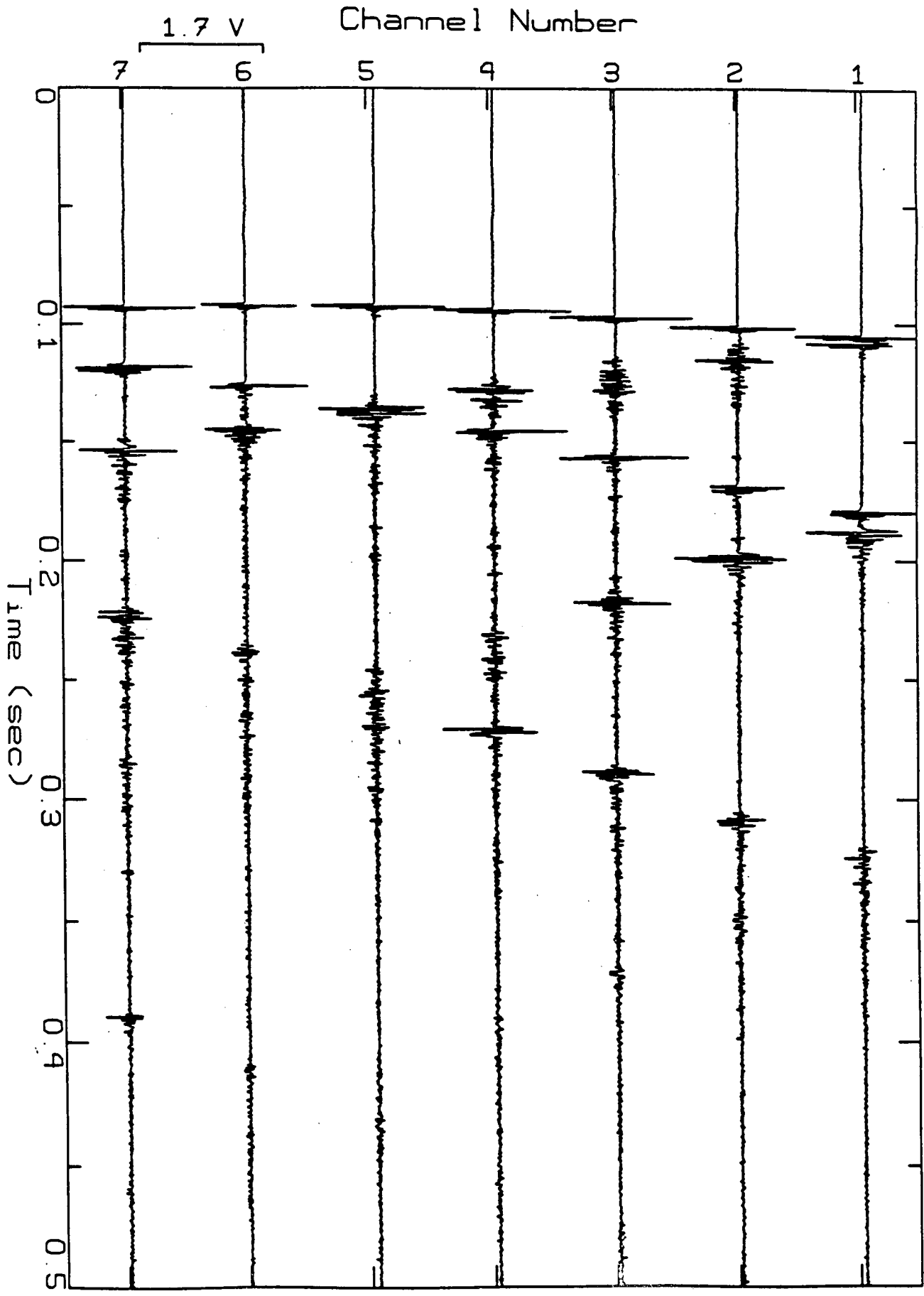
Spectra of 1431m Range Source
Source Depth 115m
Receiver Depth 150m
D (solid)   B (long dash)   S (short dash)
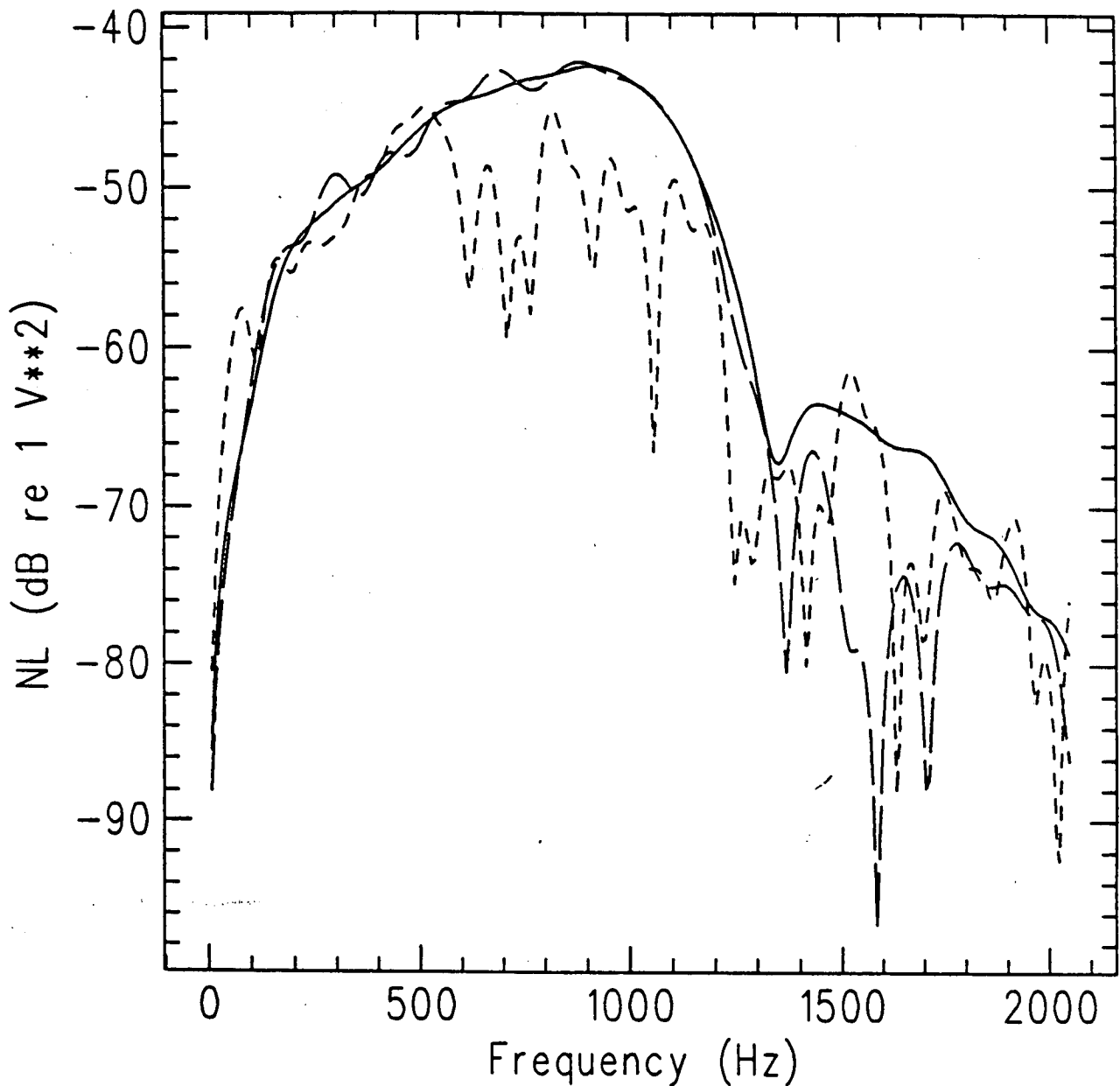
Figure 23.   Spectra of 1431 m Range Source Showing Equal Energy
in Direct Arrival and Bottom Reflection.

Figure 24. Spectra of 150 m Range Source Showing High Energy
Peak in Direct Arrival Below 200 Hz.

Time Series of Direct Arrival
Source Depth 145m
Receiver Depth 294m
150m range (solid)   1431m range (dash)
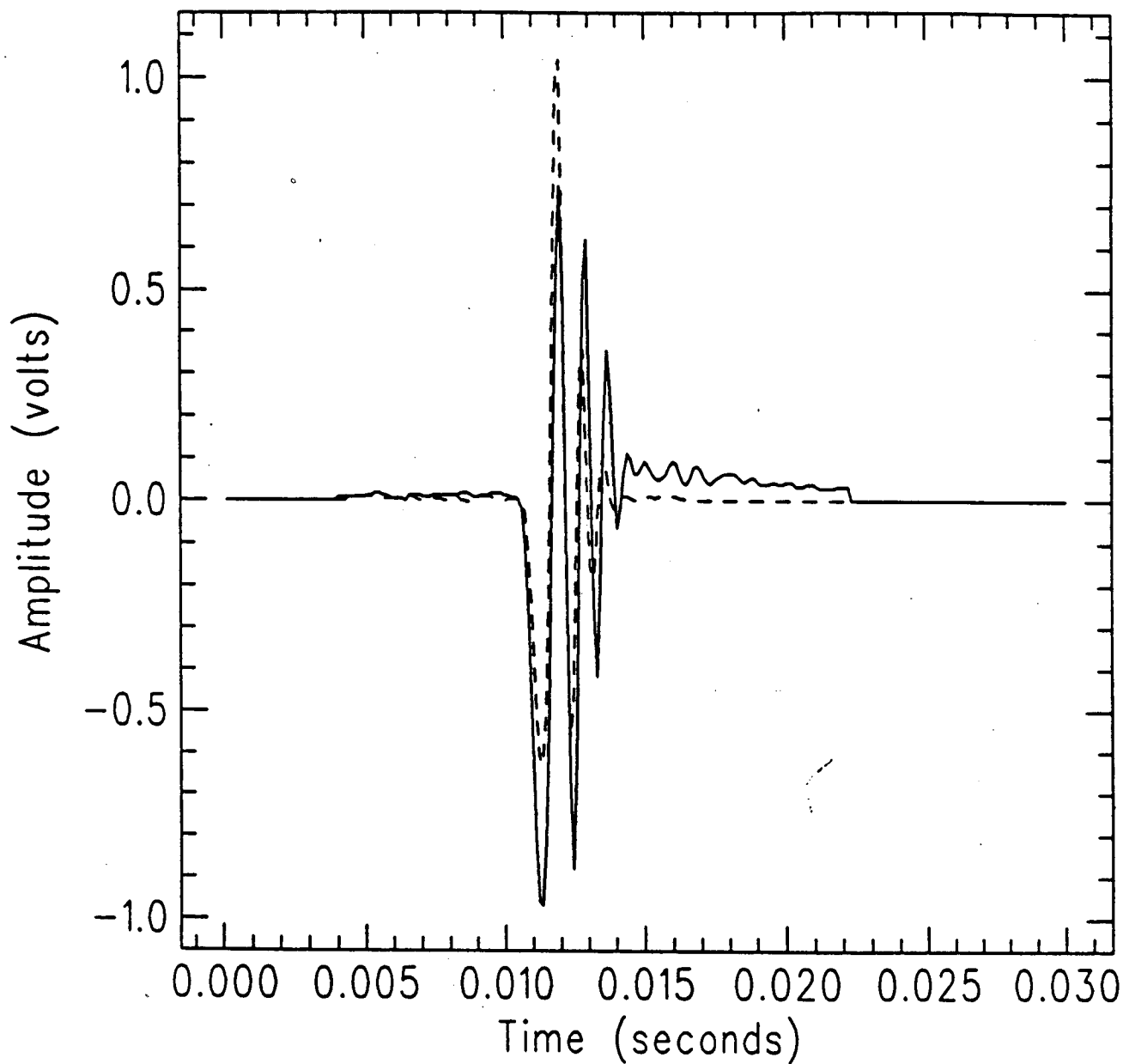
Figure 25. Time Series Showing Saturation of Direct Arrival
for 150 m Range Source.

Power Spectra for
145m Depth Source, 294m Depth Receiver
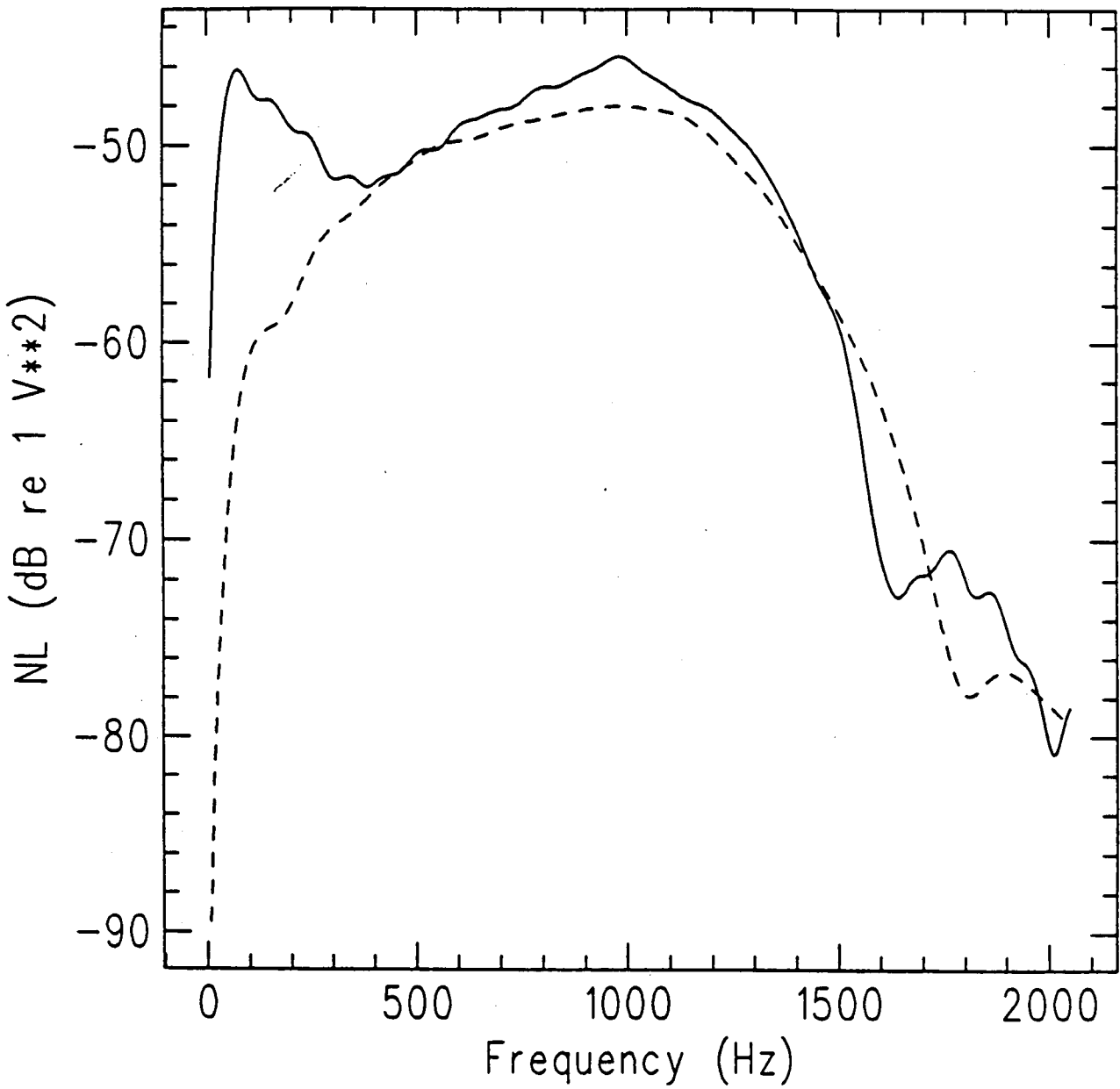150m Range (solid)   1431m Range (dash)

Figure 26.

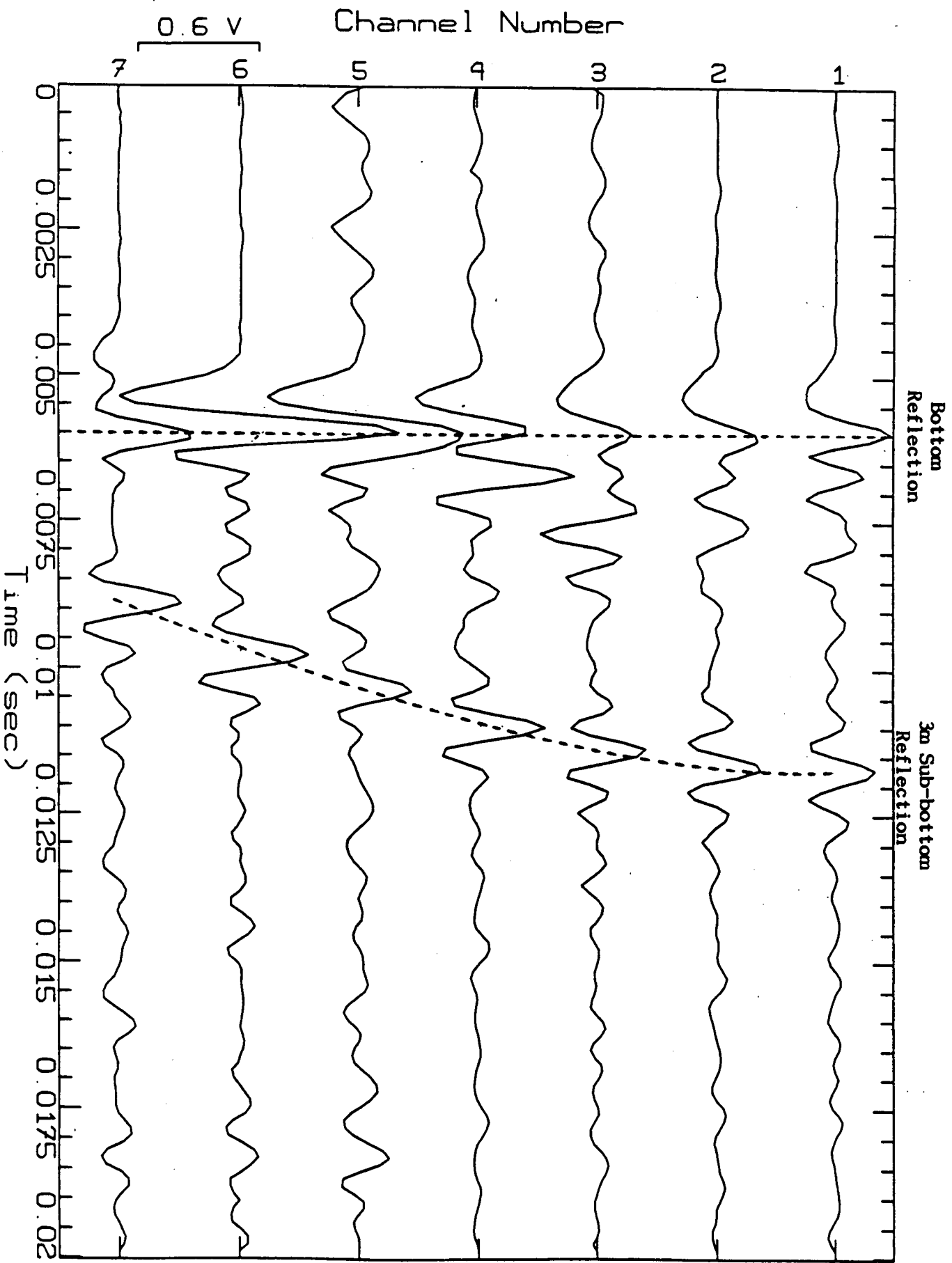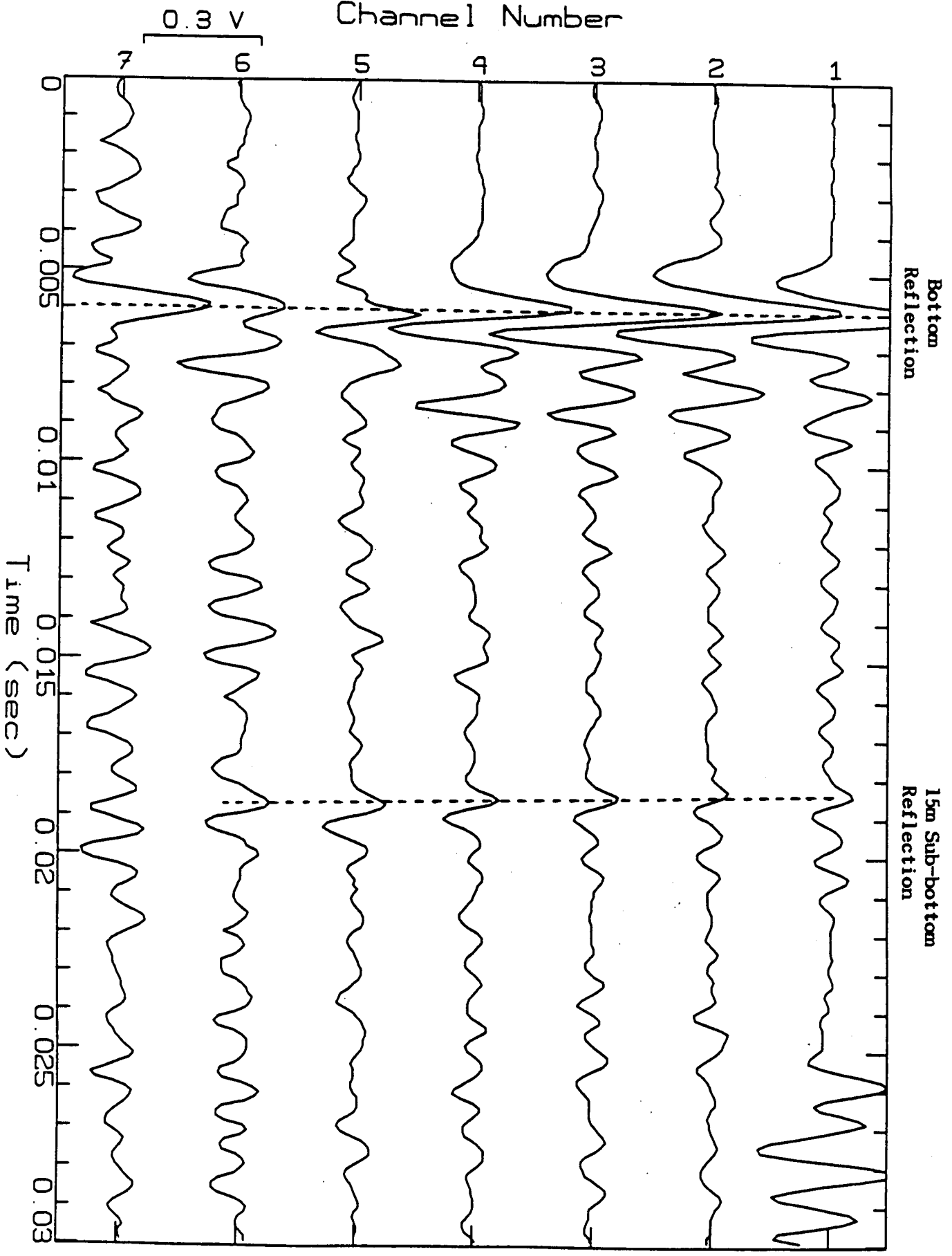Figure 27. Time Series of Bottom Reflection showing
Sub-Bottom Layer at 3 m Depth.

Figure 28. Time Series of Bottom Reflection Showing
Sub-bottom Reflection

Spectra of 1431m Range Source
Source Depth 150m
Receiver Depth 294m
D (solid)   B (long dash)   S (short dash)
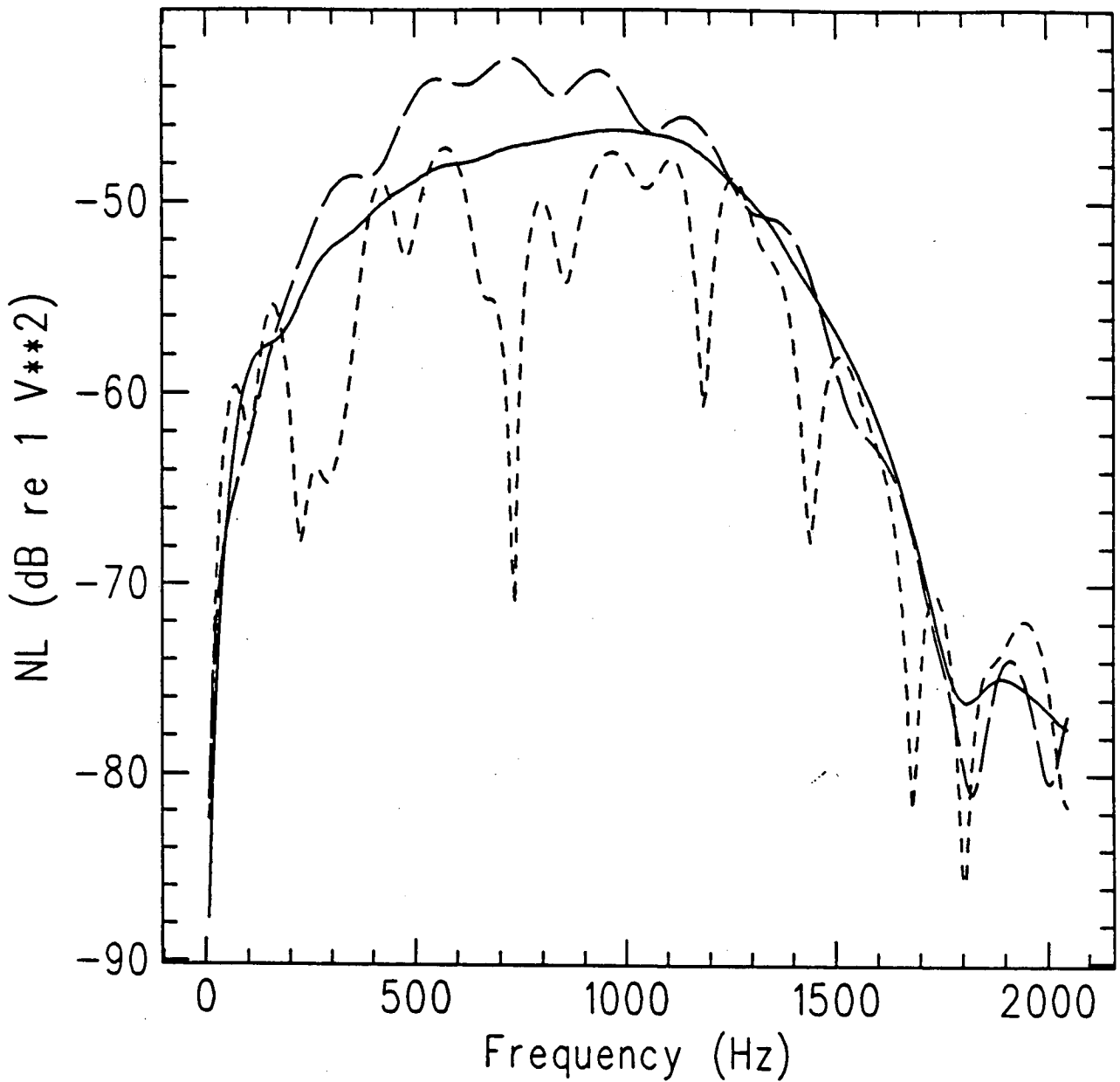

Figure 29.   Spectra for a 1431 m Range Source Showing Higher
             Power in the Bottom Reflection than Direct Arrival.

Time Series of Arrivals
Source Range 1431m
Source Depth 115m   Receiver Depth 150m
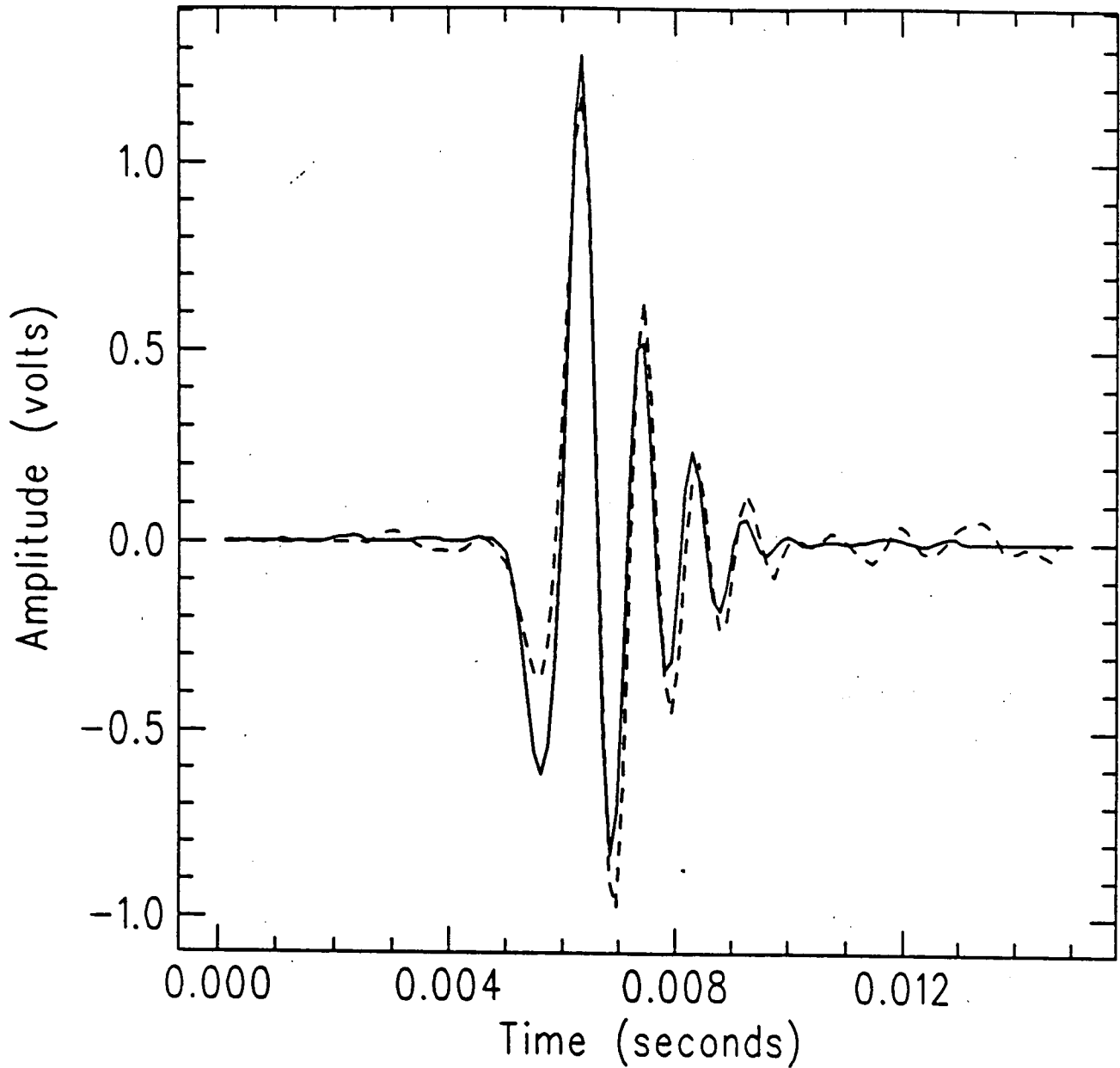## Direct (solid)   Bottom (dash)

Figure 30. Time Series of Direct Arrival and Bottom
Reflection Showing High Coherence.

REPORT NUMBER: DREP Contractors Report Series 89-28

TITLE: Arctic Ambient Noise Beamforming and Modelling

AUTHORS: Greeming, Michael

DATED: March 1989

SECURITY GRADING: UNCLASSIFIED

2 - DSIS

1 - DREA

5 - DREP

DOCUMENT CONTROL DATA

(Security classification of title, body of abstract and indexing annotation must be entered when the overall document is classified)

1. ORIGINATOR (the name and address of the organization preparing the document. Organizations for whom the document was prepared, e.g. Establishment sponsoring a contractor's report, or tasking agency, are entered in section 8.) DEFENCE RESEARCH ESTABLISHMENT PACIFIC FORCES MAIL OFFICE VICTORIA , B.C. VOS 1B0	2. SECURITY CLASSIFICATION (overall security classification of the document including special warning terms if applicable) UNCLASSIFIED

3. TITLE (the complete document title as indicated on the title page. Its classification should be indicated by the appropriate abbreviation (S,C,R or U) in parentheses after the title.)

ARCTIC AMBIENT NOISE BEAMFORMING AND MODELLING (U)

4. AUTHORS (Last name, first name, middle initial)

GREEMING, MICHAEL

5. DATE OF PUBLICATION (month and year of publication of document) MARCH 1989	6a. NO. OF PAGES (total containing information. Include Annexes, Appendices, etc.) 43	6b. NO. OF REFS (total cited in document) 2

7. DESCRIPTIVE NOTES (the category of the document, e.g. technical report, technical note or memorandum. If appropriate, enter the type of report, e.g. interim, progress, summary, annual or final. Give the inclusive dates when a specific reporting period is covered.)

CONTRACTOR'S REPORT

8. SPONSORING ACTIVITY (the name of the department project office or laboratory sponsoring the research and development. Include the address.)

9a. PROJECT OR GRANT NO. (if appropriate, the applicable research and development project or grant number under which the document was written. Please specify whether project or grant)	9b. CONTRACT NO. (if appropriate, the applicable number under which the document was written) W7708-8-9910/01-SB
10a. ORIGINATOR'S DOCUMENT NUMBER (the official document number by which the document is identified by the originating activity. This number must be unique to this document.) CRS 89-28	10b. OTHER DOCUMENT NOS. (Any other numbers which may be assigned this document either by the originator or by the sponsor)

11. DOCUMENT AVAILABILITY (any limitations on further dissemination of the document, other than those imposed by security classification)

(X) Unlimited distribution
( ) Distribution limited to defence departments and defence contractors; further distribution only as approved
( ) Distribution limited to defence departments and Canadian defence contractors; further distribution only as approved
( ) Distribution limited to government departments and agencies; further distribution only as approved
( ) Distribution limited to defence departments; further distribution only as approved
( ) Other (please specify):

12. DOCUMENT ANNOUNCEMENT (any limitation to the bibliographic announcement of this document. This will normally correspond to the Document Availabilty (11). However, where further distribution (beyond the audience specified in 11) is possible, a wider announcement audience may be selected.)

UNLIMITED

13. ABSTRACT (a brief and factual summary of the document. It may also appear elsewhere in the body of the document itself. It is highly desirable that the abstract of classified documents be unclassified. Each paragraph of the abstract shall begin with an indication of the security classification of the information in the paragraph (unless the document itself is unclassified) represented as (S), (C), (R), or (U). It is not necessary to include here abstracts in both offical languages unless the text is bilingual).

ON PAGE 1 OF REPORT

14. KEYWORDS, DESCRIPTORS or IDENTIFIERS (technically meaningful terms or short phrases that characterize a document and could be helpful in cataloguing the document. They should be selected so that no security classification is required. Identifiers, such as equipment model designation, trade name, military project code name, geographic location may also be included. If possible keywords should be selected from a published thesaurus. e.g. Thesaurus of Engineering and Scientific Terms (TEST) and that thesaurus-identified. If it is not possible to select indexing terms which are Unclassified, the classification of each should be indicated as with the title.)

ARCTIC ACOUSTICS, UNDERWATER SOUND, AMBIENT NOISE,
ICE CRACKING. SOURCE DIRECTIONALITY, SOURCE DISTRIBUTION,
SOURCE LOCALIZATION .